Photo-controlled bio-mimicking dry adhesive

by

Pamela Tannouri

M.Sc., Institut National de Recherche Scientifique, 2012

B.Sc., University of Ottawa, 2009

Project Submitted in Partial Fulfillment of the
Requirements for the Degree of
Master of Engineering

in the
School of Engineering Science
Faculty of Applied Sciences

SIMON FRASER UNIVERSITY

Spring 2016

Approval

Name: **Pamela Tannouri**

Degree: **Master of Engineering**

Title: ***Photo-controlled bio-mimicking dry adhesive***

Supervisory Committee: **Chair:** Dr. Ivan Bajić
Graduate Program Committee Chair

Dr. Carlo Menon
Senior Supervisor
Associate Professor, PEng

Dr. Teresa Cheung
Supervisor
Assistant Professor

Date Defended/Approved: January 29, 2016

Abstract

The goal of this work is to develop a photo-switchable dry adhesive. Spiropyran doped PDMS polymer was moulded into biomimetic mushroom-shaped fibrillar adhesive microstructures characterized using a variety of measurement techniques and compared with a flat control surface made of the same material. Using UV light to generate charged merocyanine molecules within 'mushroom'-shaped micro-structured PDMS films enhanced the adhesion of the film to glass surfaces. The strength of the dry adhesive property can be lowered back to the original state using visible light. Quick and efficient switching in the polymer was observed. Integrating this molecule increased normal adhesion of unstructured samples by a factor of ~4 when the polymer was in the neutral spiropyran form and ~5 for the merocyanine zwitterionic isomer, which demonstrated that control over the adhesion strength was possible. Surface charge and contact angle measurements further confirmed the proper functionality of the switch inside the PDMS polymer.

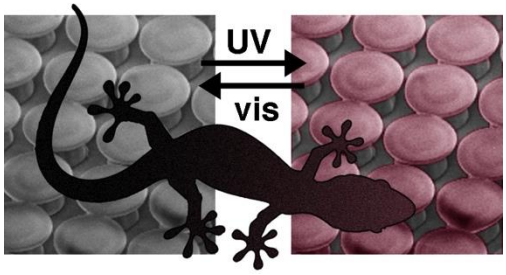

Keywords: Gecko adhesive; adhesion; micro-structures; replica moulding; photo-switching; photochemistry

To my dearest grandmother…

Acknowledgements

I was fortunate to have two inspiring supervisors who provided continuous support, valuable guidance, and remained patient throughout my studies. I wish to express my sincerest gratitude to my supervisors Professor Menon and Professor Branda, whose complementary styles have helped me excel in my studies. I can't thank them enough for giving me the opportunity to work with their group; I have learned so much from the experiences I've gained. I'd would also like thank the members of their groups for their support throughout the entire project: Jeff Krahn, Khaled Arafeh, Scott Beaupré, Yasong Li, Amir Asadirad, Tony Wu, Danielle Wilson, Kailey Wright, and Sandeep Kaur. They were all always happy to lend a helping hand, and without them, none of my accomplishments would have been possible.

This research was supported by the Natural Sciences and Engineering Research Council (NSERC) of Canada and the Canada Research Chairs Program. This work made use of 4D LABS shared facilities supported by the Canada Foundation for Innovation (CFI), British Columbia Knowledge Development Fund (BCKDF) and Simon Fraser University.

Table of Contents

List of Tables

List of Figures

Chapter 1. Introduction

The purpose of this report is to document the development of a photo-switchable dry adhesive. This chapter introduces the motivation for this objective and presents the documentation outline.

1.1. Motivation

Why photo-switchable dry adhesives?

Adhesives offer a versatile and cost effective method of binding various materials together [1, 2]. Depending on the application, clean and reusable attachment may be required, in which case, a dry adhesive in necessary. Unlike wet adhesives, which are rarely reusable since their surfaces tend to become contaminated and jeopardized due to their tacky nature, dry adhesives do not need any moisture to bind, avoiding residue and keeping the surfaces in their original condition [3]. Dry adhesives also work at a range of temperatures and pressures [4]. This behaviour is especially desirable for high-tech industries, robotic applications, biomedical dressings and devices, removable signs and labels, and many other environments of use where reusable tapes can be applied.

Effective dry adhesives rely on two factors: 1) a high degree of electrostatic interactions between the two surfaces in contact with each other [5], and 2) the fact that splitting the contact between the surfaces into finer sub-contacts increases adhesion. This latter factor is best described by the Johnson–Kendall–Roberts (JKR) model [6], which states that small fibrillar structures are less sensitive to flaws and stress concentrations, and enhance adhesion by facilitating good contact and improving compliance with surface roughness. This adhesion enhancement can also be attributed to a crack-trapping mechanism as described by [7].

Following these discoveries, several groups were inspired by the micro- and nano-scale fibrillar structures found in many ‘wall climbers’ such as the gecko lizard [8], and the development of new artificial structured materials for use as dry adhesives started growing [9]. Figure 1.1 demonstrates the intricate structures in the extremities of various ‘wall climbers’ [10].

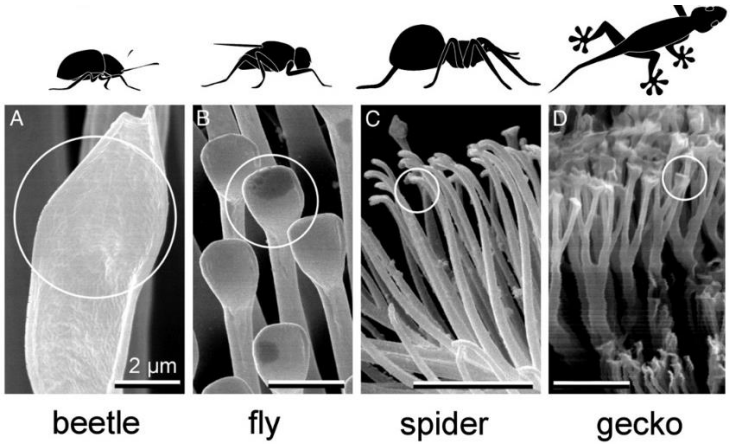

Figure 1.1. Fibrillar structured extremities (terminal elements circled) in various ‘wall climbers’ [10].

Furthermore, the ability to effectively bind two surfaces together and then separate them, repeatedly and on-command, is a highly desirable property. Introducing a control mechanism into man-made adhesives will help overcome the fact that while they are very strong, they do not detach easily without damaging the substrate surface. Fortunately, smart dynamic materials are now making it possible to have precise control over specific physical properties. These materials can reversibly respond in a defined manner to external stimulus such as light irradiation [11-13] electrical potential [14, 15], temperature [16-19], solvent [20] and pH [21], thus activating and deactivating the desired property, which is adhesion in this case.

Light is a particularly appealing stimulus to control molecular structure and the function of materials containing them. It can be tuned and focused to deliver specific wavelengths when and where it is needed. It also has low thermal effects if appropriate wavelengths and intensities are used [22], and no chemical contaminants [23].

Although photochemistry has been explored for a wide range of photoactive compounds, the design and fabrication within materials, such as polymers remain major challenges and require in depth understanding of polymer engineering, interfacial properties and surface science. Thus, we decided to first demonstrate the light-induced, reversible changes in dry adhesive properties by simply doping a photo-responsive chromophore into silicone (PDMS). While future generations of examples will have the compounds directly anchored to the polymer backbone, the doping method avoids the challenges in synthesizing complex co-polymers and the fact that these co-polymers may not have the beneficial adhesive properties of the well-studied PDMS ones.

1.2. Report Outline

Now that that it is understood why photo-controlled adhesives should be of interest, the innovative approach to solve this challenge will be presented.

This report will be organized in the following manner:

Chapter 2 provides a brief literature review, required to understand existing solutions for dry adhesives and the potential available photochrome, and to guide the way to an innovative approach. This will support the choices made in terms of materials, structures and stimulus used to overcome various challenges, and give an overview of the proposed solution.

Chapter 3 details the synthesis of materials, sample fabrication process, as well as characterization methods used to create and test the photo-controlled adhesive.

Chapter 4 reveals the results acquired and discusses their significance.

Chapter 5 presents the conclusion of this report and explores the potential for future work.

Chapter 2. Project Overview

This project touches on two major research fields: (1) synthetic dry adhesives and (2) photo-controlled materials. A brief literature review on both subject matters will be presented to highlight the general challenges faced in their respective areas. Following, the proposed innovative approach to overcome these challenges is described.

2.1. Background

2.1.1. Synthetic Dry Adhesives

The founding mechanism of dry adhesives is mainly attributed to Van der Waals forces [24, 25], resulting in dipoles between the two surfaces in contact. This phenomenon can be explained by the principles of contact mechanics; according to which splitting the contact into finer sub-contacts increases adhesion, most commonly described by the Johnson–Kendall–Roberts (JKR) theory model [26]. Accordingly, small fibrillar structures are less sensitive to flaws and stress concentrations, and enhance adhesion by facilitating good contact and improving compliance. Moreover, this adhesion enhancement can also be attributed to a crack-trapping mechanism [7, 27-28].

Once these mechanisms were understood, scientists starting turning to nature for inspiration. Various types of structures to mimic those found in wall climbing creatures were developed, made of different polymers [29, 30], carbon nanotubes [31, 32], amongst numerous others [33-38], which have successfully demonstrated enhanced adhesion.

In order to obtain the most efficient artificial dry adhesive, structural features (e.g. size and shape) should be carefully optimized [39-46]. It is important to note that the fabrication becomes significantly more difficult with the decreasing fibre diameter (i.e. increasing the number of fibres per area) for improving adhesion. Fortunately, studies have shown that the shape of the fibre tip is far more dominant when determining maximum adhesion of synthetic structures [40]. Mushroom shaped structures have been selected for this project as these have been shown to be some of the most effective in dry

adhesive films [71]. Figure 2.1 depicts a scanning electron microscope (SEM) image of a mushroom shaped PDMS adhesive sample fabricated using replica moulding.

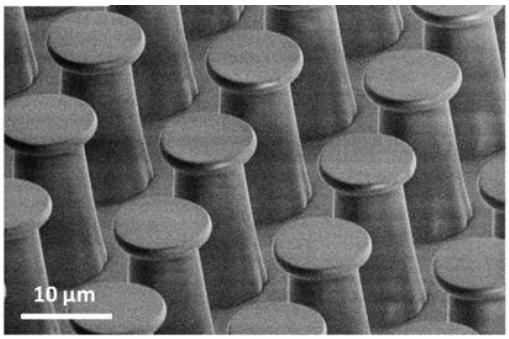

Figure 2.1. PDMS dry isotropic dry adhesives with symmetric caps produced in photoresist moulds. [71]

2.1.2. Photo-controlled Materials

Among the several forms of stimulus that can influence the state of a material, light has numerous advantages [22, 23, 47-50]; it can be delivered with very high spatial and temporal precision, low thermal effects, no chemical contaminants, and selection of any wavelength of light. Consequently, various photo-switchable molecules: azobenzenes [51, 52], stilbenes [53, 54], spiropyrans [55-57], diarylethenes [58, 59], fulgides [60, 61] and others [62, 63], have been widely explored and applied for the creation of light-responsive systems and materials. Each of these photoswitches has its own advantages and disadvantages.

Of the several known photo-responsive molecules, the choice to employ spiropyrans in our studies was based on their undergoing reversible ring-opening/ring-closing reactions between neutral and zwitterionic (merocyanine) isomers when exposed to UV and visible light (Figure 2.2) [64]. A zwitterion is a molecule that has a distinct positive and negative change distribution although it has an overall net neutral charge. These photochromic compounds have been incorporated into a wide range of materials, including polymeric matrices [65], liquid crystals [66], surface bound monolayers [67] and Langmuir-Blodgett films [68]. Despite having some performance limitations compared to other photochromic families such as thermal back reactions and often low quantum yields, the significant change in charge between their isomers should have the largest effect on

the behaviour of the dry adhesive, given that these adhesives rely primarily on electrostatic forces with the substrates.

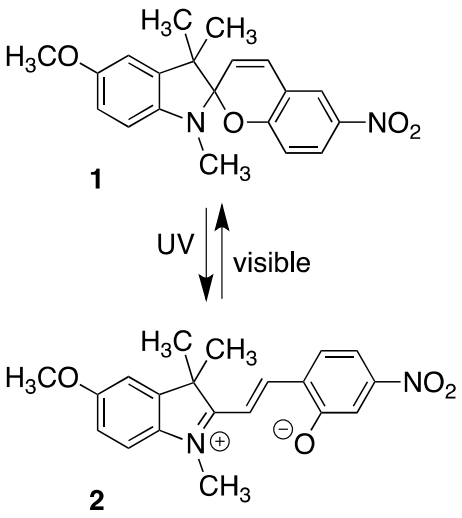

Figure 2.2. The photo-induced ring-opening and ring-closing of the photochromic spiropyran (1) and merocyanine (2) used in these studies.

2.2. Foreground

Having studied the previous works accomplished enables us to propose a feasible solution for developing a photo-switchable dry adhesive. In this report, we propose a spiropyran doped PDMS polymer moulded into biomimetic mushroom-shaped fibrillar adhesive microstructures.

This report is an introduction to the study on the integration of spiropyran in micrometer-scale structures for the control and advancement of dry adhesives synthesized from silicone polymer Polydimethylsiloxane (PDMS). Initially PDMS (Sylgard 184, 10:1 base polymer to curing agent ratio) is doped with 0.25% SP to investigate and characterize its new features since, to the best of our knowledge; this study has never been done before. In this work, we explore the effects on the surface properties of the adhesive polymer in order to understand the fundamental interaction dynamics. Experimental results of effects on normal adhesion, the ultraviolet-visible absorption spectra, the surface energy and charges of the switchable adhesive polymer are

presented. In the future, the goal would be to covalently attach the SP molecule to the PDMS backbone and run similar studies, since in theory this should increase the apparent desired properties.

Chapter 3. Materials and Methods

This chapter presents the details the synthesis of spiropyran, sample fabrication process, as well as the characterization methods used to create and test the photo-controlled adhesive.

3.1. Synthesis of Materials

3.1.1. General

All solvents and reagents used for synthesis, chromatography, UV-vis absorption spectroscopy and photolysis studies were purchased from Aldrich or Fisher and used as received, unless otherwise noted. Solvents used for NMR analysis were purchased from Cambridge Isotope Laboratories and used as received. Column chromatography was performed using silica gel 60 (230–400 mesh) from Silicycle Inc. The Sylgard 184 Silicone Elastomer Kit was purchased from Dow Corning and used as received.

3.1.2. Instrumentation

^{1}H NMR and ^{13}C NMR characterizations of all photo-responsive compounds and synthetic precursors were performed on either a Bruker AVANCE 500 TXI inverse ^{1}H/^{13}C/^{19}F instrument working at 500.19 MHz for ^{1}H and 125.78 MHz for ^{13}C or a Bruker AVANCE 400 BBOF instrument with direct probe working at 400.13 MHz for ^{1}H and 100.62 MHz for ^{13}C. Chemical shifts (δ) are reported in parts per millions (ppm) relative to tetramethylsilane (TMS) using the residual solvent peak as a reference standard. Coupling constants (J) are reported in hertz (Hz). Multiplicities are reported as s = singlet, d = double, t = triplet, q = quartet, m = multiplet. UV-vis absorption spectroscopy was performed using a Varian Cary 300 Bio Spectrometer. Fluorescence measurements were performed using a Cary Eclipse Fluorimeter-T. Infrared (IR) spectra were acquired on a Bomem (Hartmann & Braun, MB-Series) spectrometer. High-resolution mass spectra for the compounds were obtained using an Agilent 6210 TOF LC/MS (ESI+). Contact angle measurements were performed using a contact angle goniometer (OCA 15 Surface

Analysis Tool). Adhesive strength was tested using a custom apparatus consisting of a hemispherical glass probe tip (6 mm diameter) attached to a tension and compression load cell (FUTEK LRF400, 2.2 lb). The load sensor was connected to a 24-bit amplifier (FUTEK USB210) and positioned with a linear motorized stage (Zaber Technologies T-LS28-SMV). The reading and positioning was controlled using a custom script written in LabVIEW software (National Instruments).

3.1.3. Photochemistry

All ring-closing reactions were carried out using light source from a lamp used for visualizing TLC plates at 365 nm (Spectroline ENF-260C, 3.5 $mWcm^{-2}$). The ring-opening reactions were performed using the light of a 300 W halogen photo- optic source passed through a 530 nm cut-off filter to eliminate higher energy light.

3.1.4. Synthetic Methods

Figure 3.1 depicts the overview of the synthetic methods used to create the spiropyran photochrome.

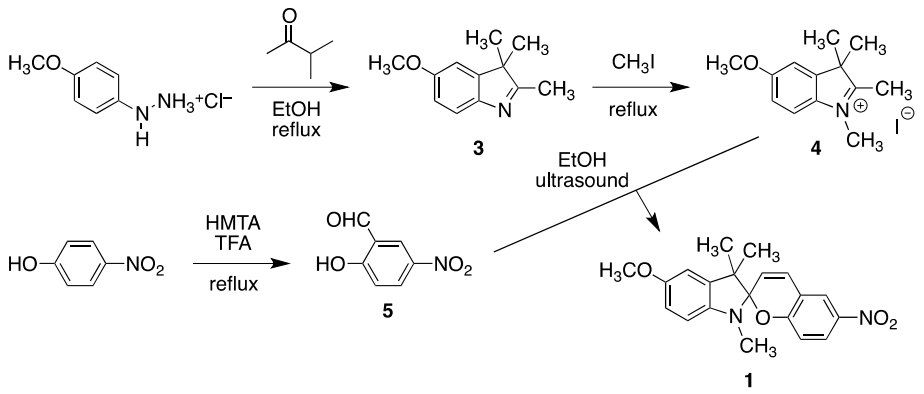

Figure 3.1. Overview of the synthetic methods used to create the spiropyran photochrome. [83]

Synthesis of 5-methoxy-2,3,3-trimethyl-3H-indole (3).

Followed according to [69]. A stirred solution of (4-methoxy)-phenylhydrazine hydrochloride (2.00 g, 11.45 mmol) in anhydrous EtOH (60 mL) was treated with 3-methyl-2-butanone (1.08 g, 12.59 mmol) at room temperature. The mixture was heated to reflux under a nitrogen atmosphere for 18 h, at which time the heat source was removed, the mixture was allowed to cool to room temperature and the solvent was removed under reduced pressure. Purification by column chromatography on silica gel (2:1 hexanes:EtOAc) afforded 1.98 g (91%) of **3** as an orange crystalline solid.

m.p. = 53–56 °C. ^{1}H NMR ($CDCl_3$, 400 MHz): δ 7.41 (d, J = 8.4 Hz, 1H), 6.82–6.78 (m, 2H), 3.81 (s, 3H), 2.22 (s, 3H), 1.27 (s, 6H). ^{13}C NMR ($CDCl_3$, 400 MHz): δ 186.03, 158.15, 147.48, 120.27, 112.24, 108.37, 55.92, 53.98, 23.45, 15.51.

Synthesis of 5-methoxy-1,2,3,3-tetramethyl-3H-indolium iodide (4).

Followed according to [69]. A stirred solution of 5-methoxy-2,3,3-trimethyl-*3H*-indole (**3**) (1.98 g, 10.46 mmol) in methyl iodide (29.71 g, 0.209 mol) was heated at reflux under a nitrogen atmosphere. After 18 h, the reaction mixture was treated with benzene (100 mL) and stirred for 30 min. The resulting brown precipitate was collected by vacuum filtration, washed with Et_2O and recrystallized from EtOH, which afforded 2.85 g (82%) of **4** as a brown crystalline solid.

m.p. = 226–228 °C. ^{1}H NMR (DMSO-d_6, 400 MHz): δ 7.82 (d, J = 8.8 Hz, 1H), 7.48 (d, J = 2.3 Hz, 1H), 7.14 (dd, J = 8.8, 2.4 Hz, 1H), 3.94 (s, 3H), 3.86 (s, 3H), 2.72 (s, 3H), 1.51 (s, 6H). ^{13}C NMR (DMSO-d_6, 400 MHz): δ 193.04, 160.50, 143.60, 135.30, 116.02, 114.10, 109.19, 56.10, 53.69, 34.73, 21.76, 13.90.

Synthesis of 2-hydroxy-5-nitrobenzaldehyde (5).

A stirred solution of 4-nitrophenol (3 g, 21.56 mmol) in trifluoroacetic acid (22 mL) was treated with hexamethylenetetramine (3.32 g, 23.72 mmol) in one portion resulting in a rapid increase in temperature. The mixture was heated at reflux and stirred under nitrogen atmosphere for 18 h, at which time it was treated with HCl (50 mL, 3M) and stirred for 2 h. The mixture was extracted with CH_2Cl_2 (3 × 50 mL). The combined organic layers

were dried over $MgSO_4$, filtered and evaporated under reduced pressure. Purification by column chromatography on silica gel (1:20 CH_3OH/CH_2Cl_2) afforded 1.8 g (50%) of **5** as a white crystalline solid.

m.p. = 126–128 °C. IR (diamond ATR): $\tilde{\nu}$ = 1657 cm^{-1} (C=O). ^1H NMR (DMSO-d_6, 400 MHz): δ 10.29 (s, 1H), 8.42 (d, J = 2.9 Hz, 1H), 8.35 (dd, J = 9.1, 2.9 Hz, 1H), 7.18 (d, J = 9.1 Hz, 1H), 3.67 (br s, 1H). ^{13}C NMR (DMSO-d_6, 400 MHz): δ 189.49, 166.10, 140.24, 131.16, 124.84, 122.65, 118.91. HRMS (ESI+) *m/z* calculated for $C_7H_6NO_4$ ($M+H^+$) 168.0291, found 168.0288.

Synthesis of 5'-methoxy-1',3',3'-trimethyl-6-nitrospiro[chromene-2,2'-indoline] (1).

Followed according to [70]. A stirred solution of 5-methoxy-1,2,3,3-tetramethyl-3H-indolium iodide (**4**) (1.42 g, 4.29 mmol) and 2-hydroxy-5-nitrobenzaldehyde (**5**) (0.72 g, 4.29 mmol) in anhydrous EtOH (50 mL) was treated with piperidine (0.47 g, 5.57 mmol) at room temperature. The mixture was degassed and sonicated at 35 kHz under a nitrogen atmosphere. After 2 h, the solvent was evaporated under reduced pressure. Purification by column chromatography on silica gel (3:1 hexanes: EtOAc) afforded 1.27 g (84%) of **1** as a purple solid.

m.p. = 226–228 °C. IR (diamond ATR): $\tilde{\nu}$ = 1472, 1332 cm^{-1} (N-O). ^1H NMR ($CDCl_3$, 400 MHz): δ 8.00–7.98 (m, 2H), 6.90 (d, J = 10.3 Hz, 1H), 6.75 (d, J = 10 Hz, 1H), 6.73–6.70 (m, 2H), 6.45 (dd, J = 5.5, 3.5 Hz 1H), 5.84 (d, J = 10.3 Hz, 1H), 3.78 (s, 3H), 2.68 (s, 3H), 1.27 (s, 3H), 1.18 (s, 3H). ^{13}C NMR ($CDCl_3$, 400 MHz): δ 160.06, 154.35, 142.06, 141.04, 137.89, 128.37, 125.98, 121.75, 118.88, 115.60, 111.62, 109.70, 107.38, 107.02, 56.07, 52.56, 29.38, 25.98, 20.03. HRMS (ESI+) *m/z* calculated for $C_{20}H_{21}N_2O_4$ ($M+H^+$) 353.1496, found 353.1505.

3.2. Preparation of PDMS doped with 0.25 wt-% spiropyran 1.

The Sylgard 184 Silicone Elastomer Kit (Dow Corning) was used to make the PDMS by mixing the PDMS base[1] (2.8 g) and the curing agent[2] (0.28 g). This mixture was treated with a solution of spiropyran **1** (7.7 mg) in CH_2Cl_2 (2 mL) and blended well using a vortex mixer for 5 min and sonicated for an additional 5 min. The CH_2Cl_2 was removed using a rotary evaporator for 10 min at 25 °C, followed by using a vacuum pump for 20 min.

3.3. Fabrication of PDMS micro-structures

Micron-scale 'mushroom'-shaped structures were fabricated using the spiropyran-doped PDMS (0.25 wt-%) mixture described above by pouring 2 g of it onto the center of a 4-inch diameter mould made of poly(methyl methacrylate) (PMMA) substrate structured with PMGI and AZ9260 photo-resist. Figure 3.2 depicts a schematic of the SP molecule distributed along the mushroom portion of the PDMS sample. Note that the SP molecules were aimed to only be dispersed into the mushroom portion of the sample for it is these structures that interact with the surface of interest. The backing of the adhesive is simply PDMS prepared in the same fashion without the SP.

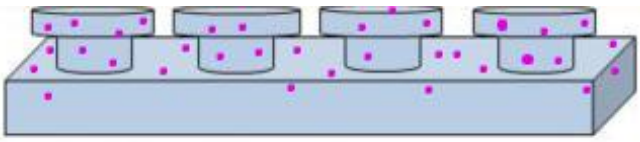

Figure 3.2. Schematic of structured SP doped PDMS sample with only top layer contains SP molecules (0.25%)

[1] This base contains dimethyl siloxane, dimethylivinyl terminated; dimethylvinylated and trimethylated silica; tetra (trimethoxysiloxy) silane; ethyl benzene.

[2] This curing agent contains dimethyl, methylhydrogen siloxane; dimethyl siloxane, dimethylvinyl terminated; dimethylvinylated and trimethylated silica; tetramethyl tetravinyl cyclotetra siloxane; ethyl benzene.

Moulds were manufactured in a similar method as previously reported [71, 72], with modifications that reliably reproduce uniform arrays of micro-structures [73-75]. The specific mould used to fabricate the micro-structures used in these experiments contained a pattern of 1.8 μm thick 'mushroom caps' having 20 μm diameters atop 12 μm 'posts' having a 12 μm diameter. After the spiropyran-doped PDMS mixture was poured into the mould, it was then spin coated at 800 RPM for 30 s to uniformly distribute the polymer mixture over the entire mould. The thin film was degassed for 20 min under low vacuum (–90 KPa) to ensure the polymer completely filled the micro-scale features of the mould and remove any trapped air. In parallel, two additional PDMS films were prepared for comparison. The first one was an unstructured film containing the same spiropyran-doped PDMS (0.25 wt-%). The second one was an unstructured film of only PDMS and no spiropyran **1**. All three sets of samples were cured in an oven at 55 °C for 3 h.[3] After cooling to room temperature, the films were layered with 5 g PDMS polymer as backing that was previously degassed to remove the trapped air induced by mixing.[4] The samples were spin coated at 800 RPM for 30 s and cured in an oven at 55 °C overnight. The films were removed from the moulds and imaged (Figure 3.3 and 3.4).

[3] The temperature was maintained below 65°C, at which temperature the spiropyran decomposes.

[4] This support layer of PDMS helps ease the demoulding process.

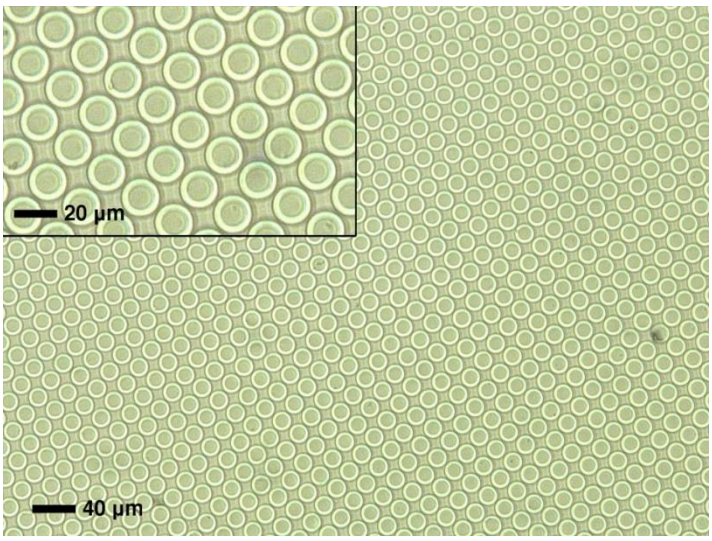

Figure 3.3. Optical microscope image of the micro-structured PDMS 'mushrooms' containing 0.25 wt-% spiropyran 1. [83]

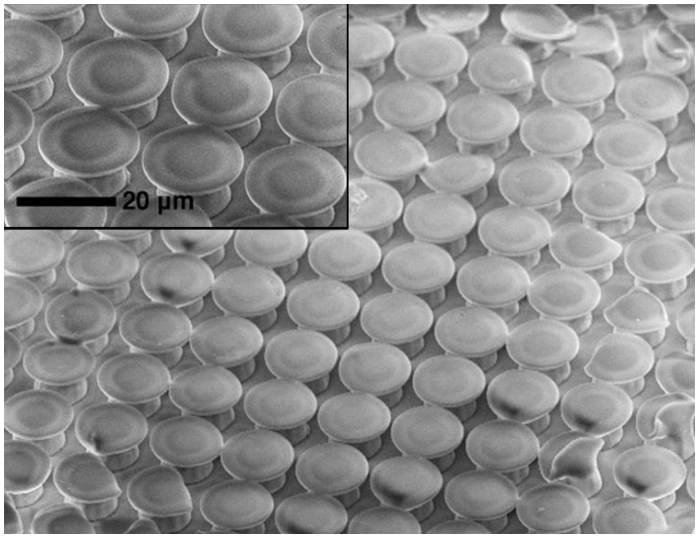

Figure 3.4. SEM images of the micro-structured PDMS 'mushrooms' containing 0.25 wt-% spiropyran 1. [83]

3.4. Experimental Methods

3.4.1. Photochemistry of spiropyran 1 – synthesis of merocyanine 2

The photochromic response is directly related to the absorption characteristics of the photochrome. The SP molecule undergoes a photo-reversible transfiguration between two thermodynamically stable photoisomers, from an electrically neutral closed spiropyran form to its zwitterionic merocyanine (MC) form, under irradiation of UV light (<450nm) (Figure 3.5). This process is reversible via exposure to visible yellow light (>530nm) or heat.

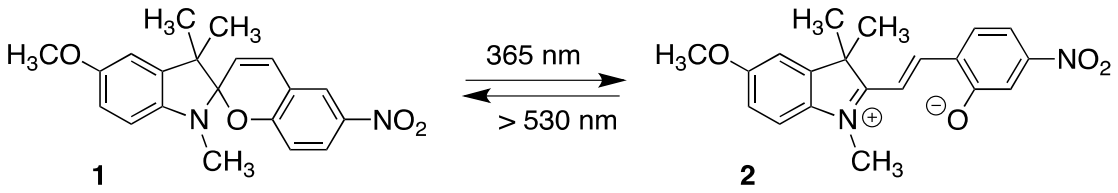

Figure 3.5. Schematic illustration of the photochromic phenomenon; spiropyran closed-ring isomers are reversibly transformed into merocyanine open-ring isomers by alternating UV and VIS irradiation.

Non-structured and micro-structured PDMS films containing spiropyran **1** (0.25 wt-%) were irradiated with 365 nm light and the absorption spectra were recorded. The exposure was continued until there were no changes in the spectra. To quantify this measure, optical absorption spectra were performed with a Cary 500 UV-VIS spectrophotometer (Varian, Inc.); untreated polymer of the same thickness was used as a reference. Samples were illuminated with visible yellow light (>530nm) for 1 min and the spectrum was scanned from 300 to 800 nm at room temperature immediately after irradiation. Following, samples were illuminated with a specific UV wavelength of 365 nm for 1 min, which activate the photochromic compound in the polymer matrix and a second spectrum was taken immediately after. The material developed a characteristic magenta color upon irradiation with UV light.

3.4.2. Surface Charge

The surface charge of a material is the number electric charges present at its interface. Since our photochromatic molecule switches from a closed neutral form to an open charged one, we expect the surface charge to change along with this switching. In order to determine the surface charge of our material, a fluorescence test was conducted on samples of 1 cm x 1 cm of each structured and flat samples, one in the closed form and one in the charged state, for a total of 4 samples. Each sample was dipped in a 1% solution of fluorescein (Na salt) in distilled water for 5mins. Next, the sample was carefully rinsed with distilled water and placed in 20 mL of 0.1% cetyltrimethylammonium chloride in distilled water, and shaken for 10 mins to desorb the dye. Then, 10% (v/v) of a 100 mM aqueous phosphate buffer, pH 8.0 was added to the remaining solution. The absorbance of the resultant aqueous solution was measured with a fluorimeter (Cary Eclipse Fluorimeter-T) at 510 nm. The independently determined extinction coefficient of fluorescein in this solution was found to be 77 $mM^{-1}cm^{-1}$ [76].

3.4.3. Contact angle measurements

Surface energy of a material can be derived from the contact angle of a liquid at an interface, using a contact angle goniometer. The contact angle (CA) can also quantify the wettability of a solid surface by a liquid via the Young equation [15, 77]. The wetting behaviour of a solid surface is an important property, and is governed by both the chemical composition and the geometrical structure of surface [78]. Here we've used the contact angle goniometer (OCA 15 Surface Analysis Tool). The OCA 15 tool is capable of determining many different properties of surfaces. It uses an electronically controlled syringe attached to the instrument in order to dispense a liquid onto a substrate. A digital video camera is used to view the substrate and liquid drop. The camera and syringe are both controlled through a software package contained on the associated PC. The SCA integrated software provides the ability to measure surface free energy, as well as dynamic and static contact angles. Water droplets were released onto the SP doped, unstructured and structured, samples. Images were acquired while the samples were in both photochromic states.

3.4.4. Adhesive strength measurements

Normal adhesion tests were performed with a custom apparatus consisting of a hemispherical glass sphere probe tip of 6 mm diameter attached to a tension and compression load cell (FUTEK LRF400, 2.2 lb). The load sensor was connected to a 24-bit amplifier (FUTEK USB210) and positioned with a linear motorized stage (Zaber Technologies T-LS28-SMV) (Figure 3.6). The reading and positioning was controlled using a custom script written in LabVIEW software (National Instruments).

Un-doped, non-structured and micro-structured pure PDMS samples were tested as reference films. The glass probe tip was cleaned before each measurement with alcohol wipes and left to dry for 10 min. Random spots on all adhesives were chosen for testing. The load cell was set to apply a preload on the sample of either 100 mN or 200 mN. An iteration is defined as one set of probing, i.e. one preload and one adhesion force measured. The goal was to collect as many number of iterations as possible in a given session with the setup.

Automated software lowered the load cell until the probe made contact with the sample; the desired force is applied, controlled through a feedback loop, and then retracted. The actual contact area of the probe tip to the film surface was approximately 3 mm^2. The force required to remove the glass tip from the surface reflects the adhesion between the two surfaces.

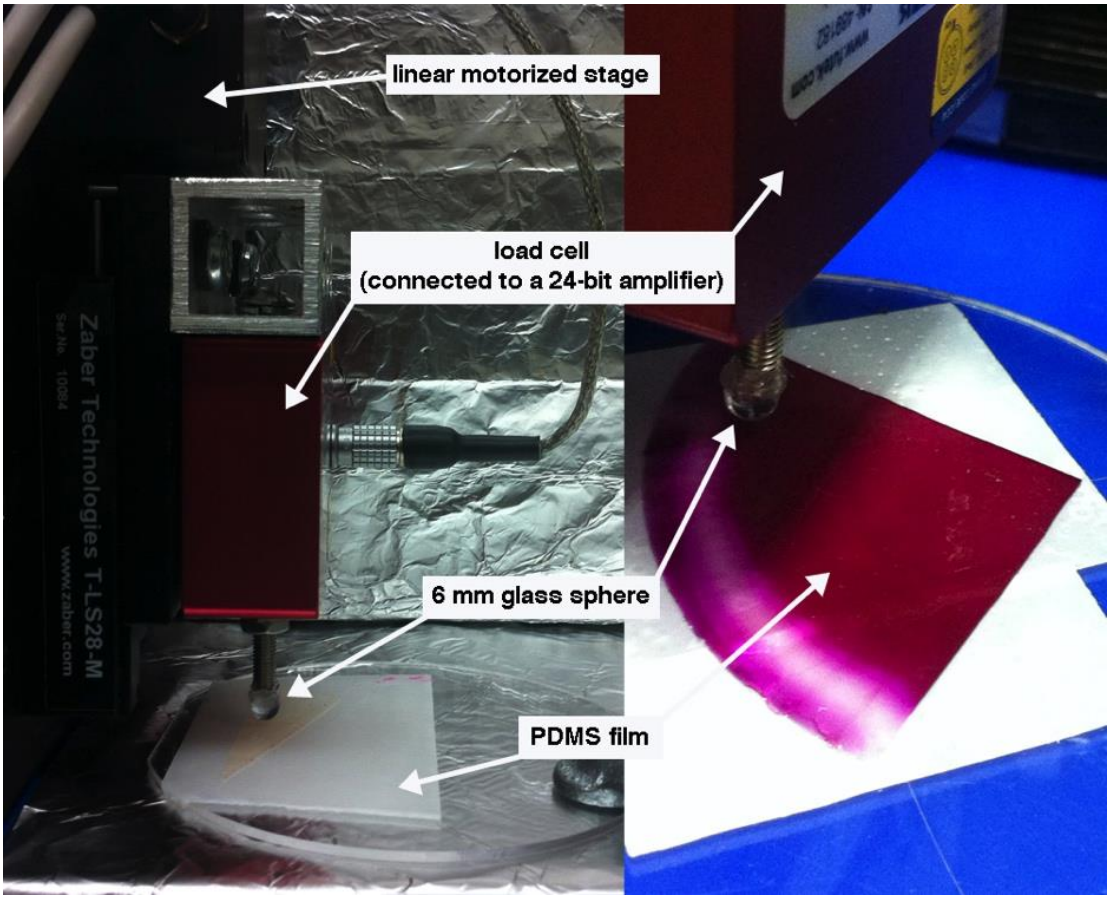

Figure 3.6. **Photographs of the measurement tool used to quantify the adhesion of the films to a glass hemispherical tip. In these experiments, the glass tip is placed in contact with the PDMS film with preload values of 100 mN or 200 mN. The force required to remove the glass tip from the surface reflects the adhesion between the two surfaces. The film in the left photograph has the photo-responsive molecule in the colorless spiropyran state (1). The one on the right is after exposure to 365 nm light for 60 s and represents the photo-stationary state containing merocyanine (2). [83]**

Chapter 4. Results and Discussion

4.1. Photochemistry of spiropyran 1 – synthesis of merocyanine 2

The photochromic behaviour of the spiropyran chromophores in the films is best shown by comparing the UV–vis absorption spectra before and after exposure to light. Non-structured films effectively demonstrate this behaviour because they do not suffer from the scattering of light observed for the micro-structured versions that complicates the spectra. The absorbance bands for the chromophores appear at the same wavelength for both types of films. The colorless, PDMS films containing 0.25 wt-% spiropyran **1** become magenta when the films are exposed to 365 nm light (Figure 4.1(b)). This color corresponds to the appearance of a band centered at 550 nm in UV-vis absorption spectrum (Figure 4.1(a)), which can be assigned to the merocyanine isomer generated from the ring-opening reaction (**1** $\rightarrow$ **2**). This band and the color of the film disappear upon exposure to light of wavelengths greater than 530 nm as the cyclization reaction (**2** $\rightarrow$ **1**) occurs when excited in this spectral region. These ring-opening/ring-closing reactions suffer from little fatigue as shown by the insignificant decrease in absorption intensity of the band corresponding to the merocyanine isomer **2** in a micro-structured film during several cycles (Figure 4.1(d)). It is important to note that the micro-structured un-doped film used as a background is likely not identical to that for the 0.25 wt-% **1** film, which introduces fluctuations in the spectral data.

Non-structured and micro-structured PDMS films containing spiropyran **1** (0.25 wt-%) were irradiated with 365 nm light and the absorption spectra were recorded. The exposure was continued for approximately 120 s, until there were no changes observed in the spectra. These spectra are shown in Figure 4.1 (a) and (d). Furthermore, ring-closing of the merocyanine back to the spiropyran is slow in both non-structured and micro-structured PDMS films. In the dark, the half-life for the decay of the absorption at 550 nm corresponding to compound **2** is 45–55 min for either film (Figure 4.2).

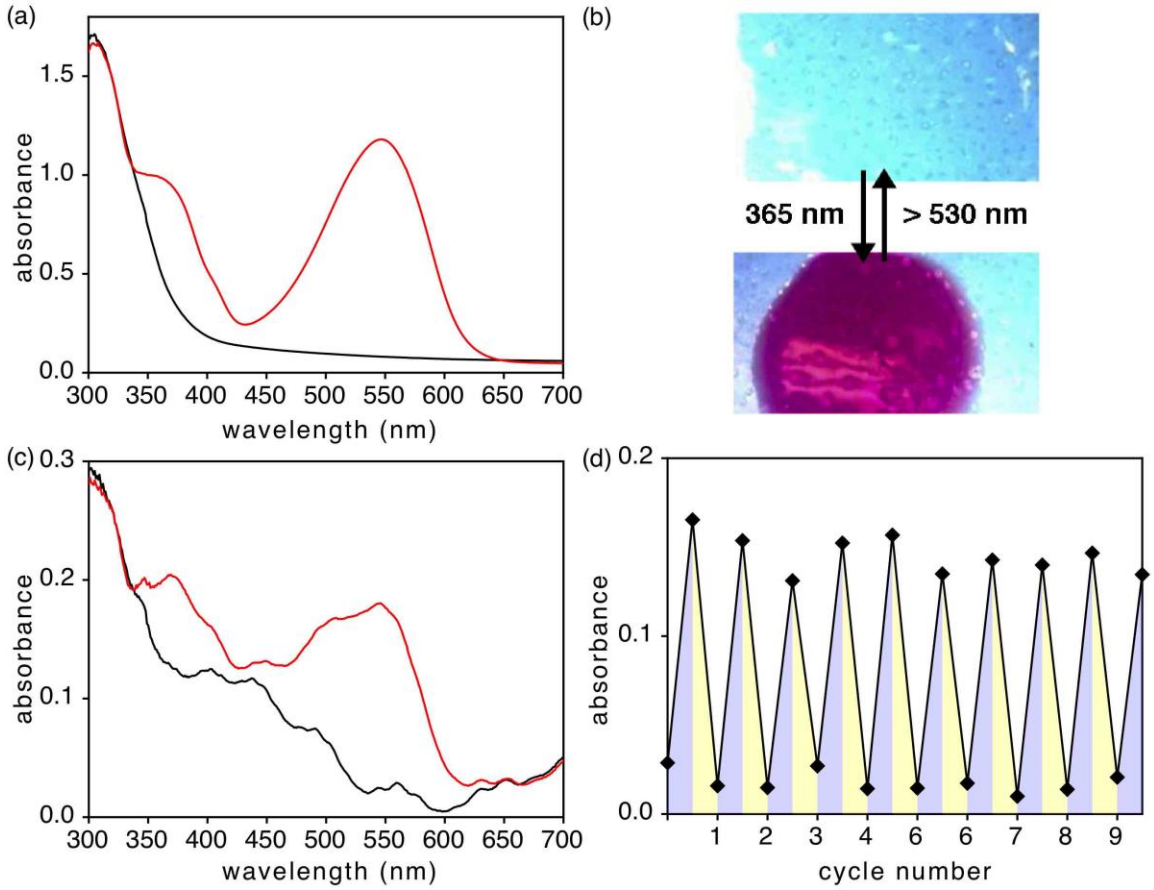

Figure 4.1. **(a) UV-vis absorbance spectra of a non-structured PDMS film containing spiropyran 1 (0.25 wt-%) before (black line) and after (red line) irradiation with 365 nm light for 5 min. (b) Photo-graphs of the same film before (top) and after (bottom) irradiation with 365 nm light for 5 min. (c) UV-vis absorbance spectra of a micro-structured PDMS film containing spiropyran 1 (0.25 wt-%) before (black line) and after (red line) irradiation with 365 nm light for 1 min. (d) Changes in the absorbance (560 nm) corresponding to the ring-open isomer (2) in a micro-structured film containing 0.25 wt-% spiropyran 1 upon alternate irradiation with 365 nm light for 120 s (non-shaded regions) and > 530 nm light for 120 s (grey shaded regions). An un-doped micro-structured PDMS film of the same thickness was used as the background reference. [83]**

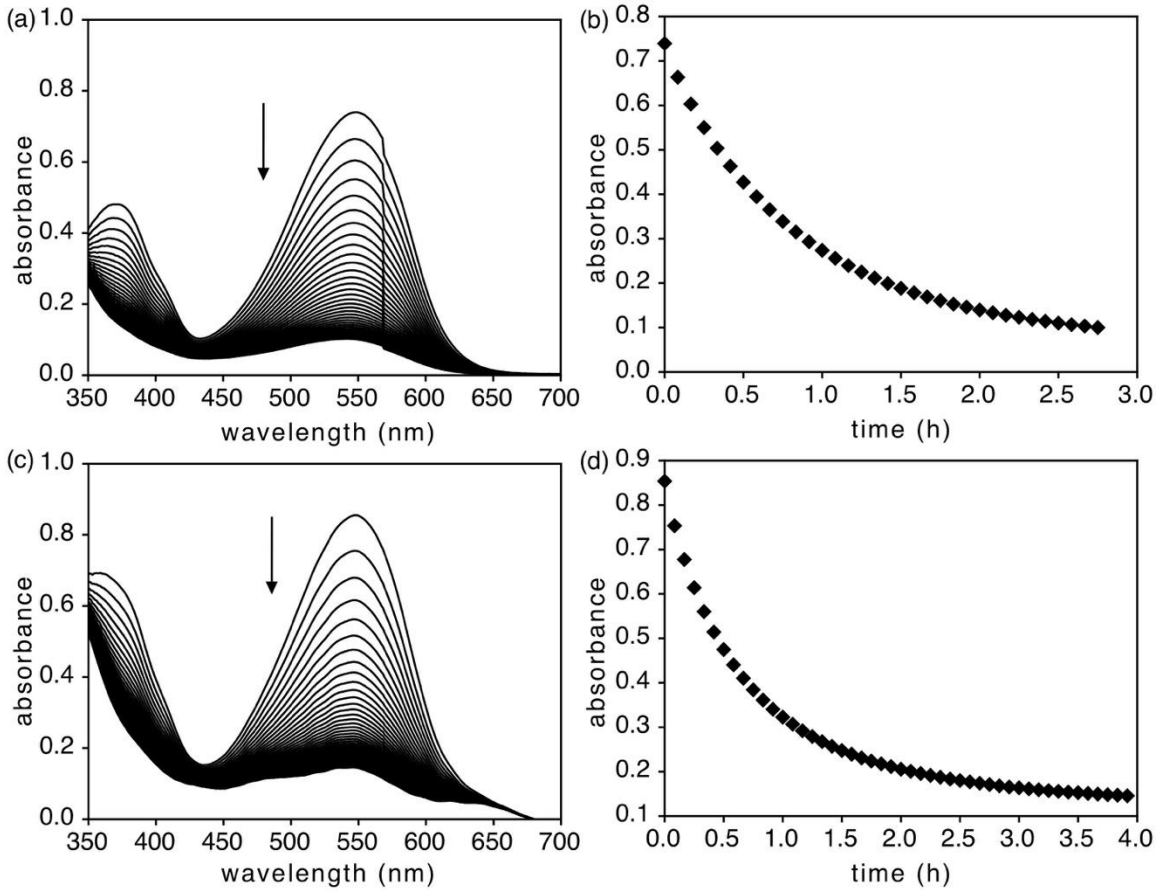

Figure 4.2. **(a) Changes in the UV-vis absorbance spectra of a non-structured PDMS film containing merocyanine 2 (0.25 wt-%) at room temperature in the dark. The photo-stationary state containing 2 was generated by irradiating the film with 365 nm light for 5 min. (b) The decrease in absorption intensity at 550 nm of the same film over time. (c) Changes in the UV-vis absorbance spectra of a micro-structured PDMS film containing merocyanine 2 (0.25 wt-%) at room temperature in the dark. The photo-stationary state containing 2 was generated by irradiating the film with 365 nm light for 5 min. (d) The decrease in absorption intensity at 550 nm of the same film over time. [83]**

4.2. Surface Charge

The absorption of samples was taken with a fluorimeter (an example is shown in Figure 4.3). The absorbance, A, is defined as: $A = log10(I_0/I_t)$, where I_0 & I_t refer to the intensity of light incident on the sample and transmitted by the sample respectively. The absorbance of a sample is related to the concentration of the absorbing species and the path length of the sample by the Beer-Lambert Law; $A = \varepsilon \cdot c \cdot l$, where ε is the molar extinction coefficient ($\mathrm{dm^3/mol \cdot cm}$), c is the concentration ($\mathrm{mol/dm^3}$) and l is the path length (cm) [79].

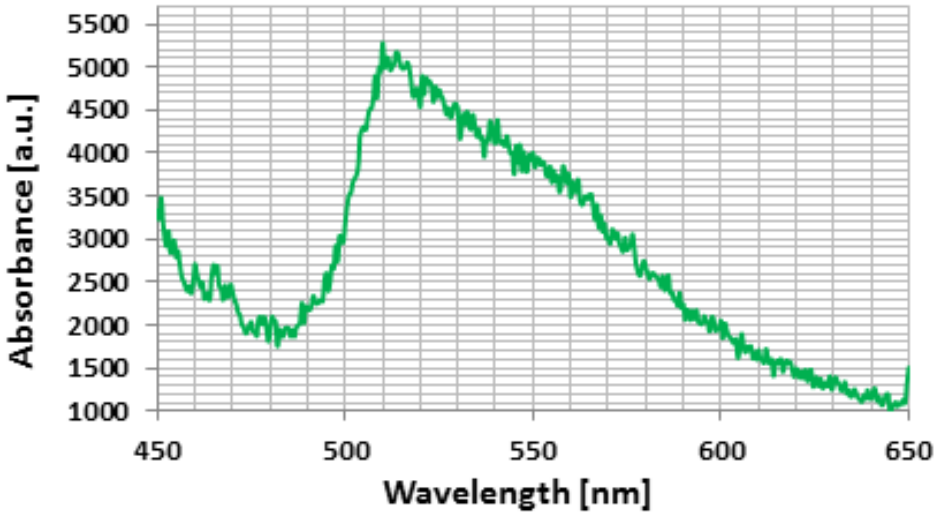

Figure 4.3. Example of fluorimeter absorbance spectrum of samples of 1 cm x 1 cm of sample dipped in a 1% solution of fluorescein (Na salt) in distilled water for 5mins, rinsed with distilled water and placed in 20mL of 0.1% cetyltrimethylammonium chloride in distilled water, and shaken for 10 mins to desorb the dye. 10% (v/v) of a 100 mM aqueous phosphate buffer, pH 8.0 was added to the remaining solution. The absorbance of the resultant aqueous solution was measured.

In this case ε = 77 $mM^{-1}cm^{-1}$, the length of the sample is the length of the cuvette; l=1cm and A is the peak absorbance. From this, we can find the concentration of charges for the sample, for the known area. For the unstructured sample a concentration of ~0.85 mMol/cm^2 is calculated for the SP neutral closed form and ~1.01 mMol/cm^2 for the MC charged open form. For the structured sample the concentrations were slightly higher due

to the increased surface area; ~0.89 mMol/cm^2 for the SP neutral closed form and ~1.16 mMol/cm^2 for the MC charged open form, indicating that as expected, that the MC open charged state has approximately 1.5 more charges than the neutral SP one.

4.3. Contact angle measurements

The entire design of the system described in this report was based on the photo-induced changes in the net charges at the surface of doped PDMS films as the photo-responsive chromophores interconvert between neutral spiropyrans and zwitterionic merocyanines, and how they will affect the electrostatic attraction at the interface of the film and substrates such as glass. The modulation of the bulk electrostatic charge at the PDMS surface was first demonstrated using UV (365 nm) and visible (> 530 nm) light to affect the 'wetting' of the PDMS films. The contact angle of water droplets resting on top of doped PDMS films (0.25 wt-% spiropyran **1**) decrease when the films are exposed to UV (365 nm) light. The 'wetting' behaviour of a solid surface is governed by both the chemical composition and the geometrical structure of microscopic features on the surface [64]. The small loading of spiropyran **1** (0.25 wt-%) will not affect the size or shape of the 'mushroom' structures. A representative example is shown in Figure 4.4 and more details are Table 4.1 ([a] The films were exposed to visible light (> 530 nm) to ensure all the photo-responsive compound was in its spiropyran (**1**) state. [b] The films were irradiated for 60 s prior to applying the water droplets.).

In the case of the non-structured films, the contact angle decreased by an average of 8° (102.3° ± 1.6° for **1** and 94.1° ± 1.0° for **2**) corresponding to an 8% change. The decrease was larger (19°) for the micro-structured films (130.8° ± 3.7° for **1** and 111.6° ± 2.0° for **2**), which corresponds to a 15% change. These results illustrate that the photo-induced ring-opening of the spiropyran **1** to its zwitterionic merocyanine counterpart (**2**) results in an increase in the hydrophilic nature of the doped PDMS films due to an increase in electrostatic charge at the interface. As expected the micro-structured films have larger contact angles than the non-structured films, which can be ascribed to the "lotus leaf effect". Introducing this control over the wettability of a material also has the potential to offer 'on-demand' self-cleaning properties [80], which will be the subject of future studies.

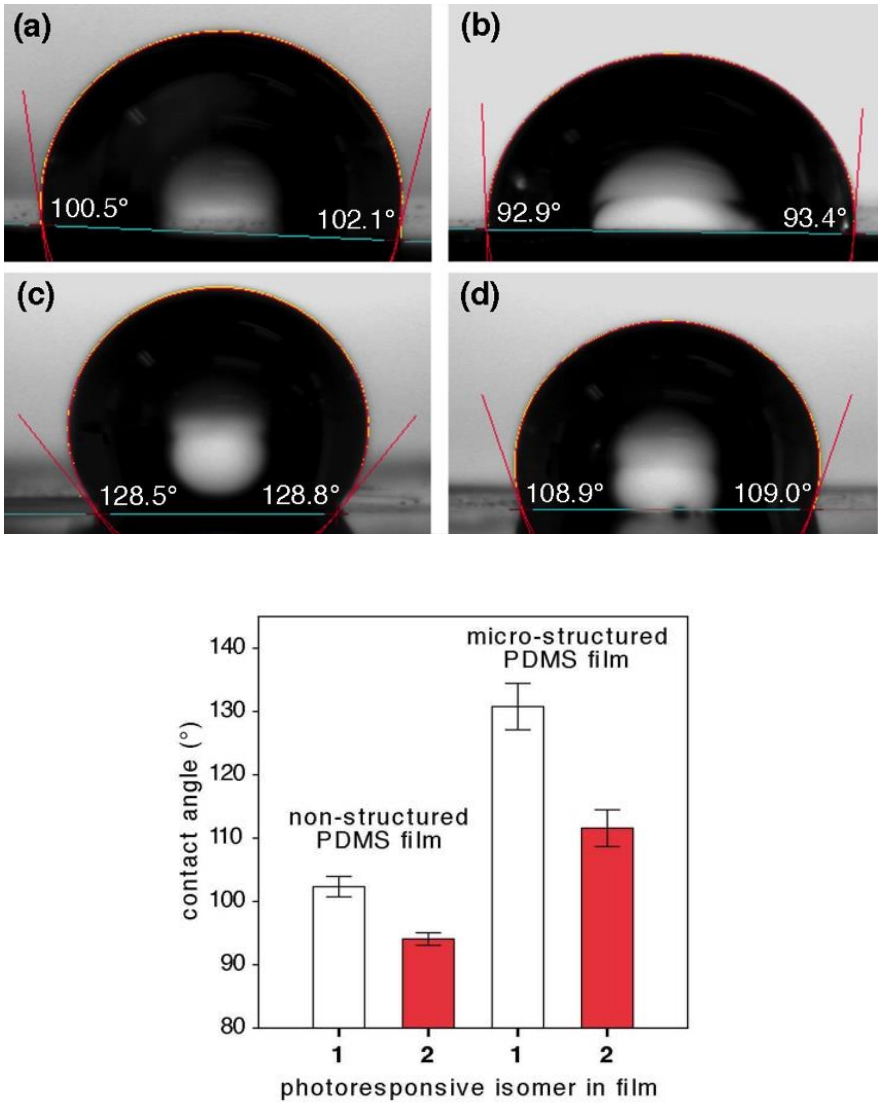

Figure 4.4. **Representative examples of contact angle measurements of a droplet of water on top of (a) a non-structured PDMS film doped with 0.25 wt-% spiropyran 1, (b) the same film after exposure to 365 nm light for 60 s, (c) a micro-structured PDMS substrate doped with 0.25 wt-% spiropyran 1, (d) the same film after exposure to 365 nm light for 60 s. The plot of the right shows the average value for all measurements (data from Table 4.1). [83]**

Table 4.1. Contact angle measurements for water droplets on top of non-structured and micro-structured PDMS films doped with spiropyran 1 (0.25 wt-%) before and after exposure to 365 nm light for 60 s. [83]

non-structured				micro-structured			
before irradiation[a] (PDMS-**1**)		after irradiation[b] (PDMS-**2**)		before irradiation[a] (PDMS-**1**)		after irradiation[b] (PDMS-**2**)	
theta L (°)	theta R	theta L (°)	theta R	theta L	theta R	theta L (°)	theta R
100.7	101.4	92.9	93.6	131.3	131.1	115.7	115.1
100.6	101.3	92.5	93.5	131.1	131.0	116.7	116.3
104.4	104.4	93.5	94.4	131.1	131.0	115.2	115.1
100.5	101.2	96.7	95.5	130.4	129.7	111.4	111.8
104.3	104.3	93.6	94.3	130.3	129.6	113.6	113.6
102.9	102.9	94.9	94.9	130.0	130.0	109.0	109.0
100.0	99.8	92.9	93.4	127.9	127.4	108.9	109.0
102.4	102.0	94.5	94.5	127.8	127.4	112.2	112.2
103.2	103.2	93.6	94.3	128.5	128.3	109.7	112.1
104.7	104.3			129.2	129.3	110.3	110.3
				128.5	128.8	109.7	112.1
				137.5	137.5	109.0	109.0
				128.5	128.8	106.9	106.9
				130.5	130.5		
				130.7	130.6		
				129.4	129.3		
				139.4	139.3		
				139.5	139.3		
				128.0	128.1		
				127.2	127.1		
average contact angles (°)							
102.3±1.6		94.1±1.0		130.8±3.7		111.6±2.	

4.4. Adhesive strength measurements

The presence of SP nanoparticles on the surface of the adhesive can in principle improve the adhesion because of the reduction of the Hamaker constant and Young's modulus [81]. A complete study of this effect is beyond the current work; however, we hope to investigate this phenomenon in the future..

The adhesion strength of the SP doped micro-structured films to glass was evaluated using the instrumentation described in the previous chapter (section 3.4.4). Un-doped, non-structured and micro-structured pure PDMS samples were tested as reference films. A glass sphere probe was lowered to make contact between the two surfaces with a specified preload force (F_p) as shown schematically in Figure 4.5 (a). Note the actual contact area of the probe tip to the film surface is approximately 3 mm^2. The force required to retract the glass tip from the film (F_a in Figure 4.5 (b)) reflects the adhesion strength between the two surfaces. It is important to note that each 'iteration' represents a single measurement of the force required to detach the probe tip from the film at the same spot, as shown in this figure (Figure 4.5 (b)). A preload force of 100 mN was used for the measurements described in this report and all adhesion strengths are reported in Tables 4.2 and 4.3. Higher values of F_p resulted in insignificant differences in F_a (see Figure 4.6 for more details. Note that the scale of figure (b) ranges from 130mN-155mN and (c) ranges from 120mN-132mN.). This could be potentially due to deformations of the sample at the higher preload force.

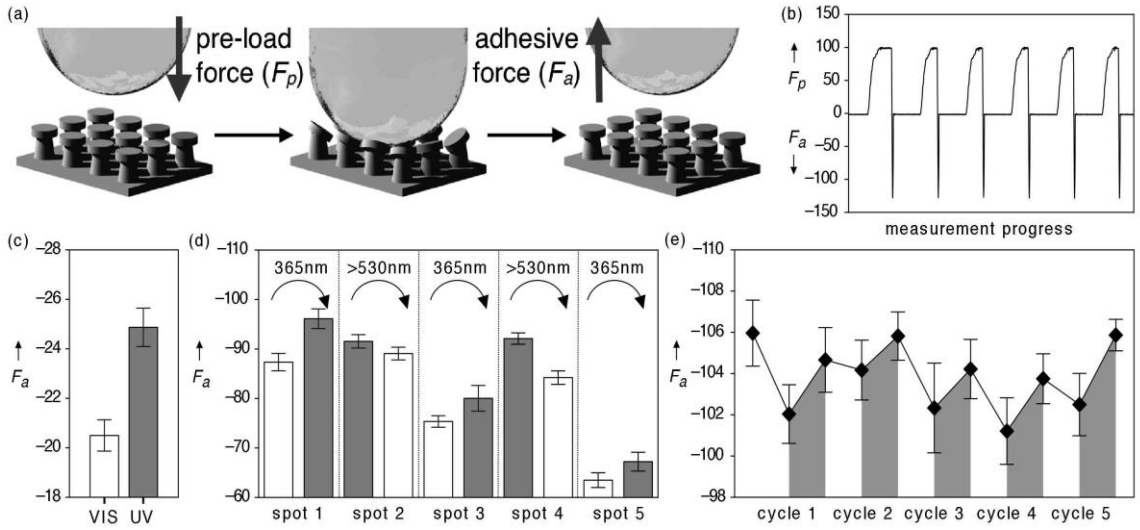

Figure 4.5. **(a) Schematic representation of how the adhesive strengths between the films and a glass sphere are measured. After a preload force (F_p) is applied, the force needed to retract the sphere from the film (F_a) reflects the adhesion between the two surfaces. (b) Representative example of macro-scale adhesion force data between a glass sphere and the micro-structured PDMS film containing spiropyran 1. (c) Average adhesion strengths for a non-structured PDMS film doped with spiropyran 1 (0.25 wt-%) before (white bar) and after (grey bar) it is exposed to UV light (365 nm) for 60 s. Each bar is the average value of F_a from at least 30 measurements at the same spot. (d) Average adhesion strengths for several spots on a micro-structured PDMS film doped with spiropyran 1 (0.25 wt-%) as the film is exposed to UV light (365 nm) and visible light (>530 nm). Each bar is the average value of F_a from at least 40 measurements. (e) Average adhesion strengths for a single spot on a micro-structured PDMS film doped with spiropyran 1 (0.25 wt-%) as it is exposed to UV light (365 nm) and visible light (>530 nm). Each bar is the average value of F_a from at least 20 measurements at the same spot. All measurements were acquired using a preload force of 100 mN. [83]**

Table 4.2. **Summary of the average adhesion strengths of non-structured PDMS films with preload forces of 100 mN and 200 mN with and without 0.25 wt-% spiropyran 1. Average values and standard deviations (SD) are reported for various spots on the sample as well as alternating visible light (>530 nm) and UV light (365 nm) cycles. [83]**

non-structured									
	non-doped					0.25 wt-% spiropyran		0.5 wt-% spiropyran	
	100 mN preload		200 mN preload			100 mN preload		100 mN preload	
	average (mN)	SD	average (mN)	SD		average (mN)	SD	average (mN)	SD
spot 1	-24.7	2.6	-31.7	3.1	spot 1 (VIS)	-20.5	0.6	-82.0	1.1
spot 2	-18.6	1.9	-22.4	2.1	(UV)	-24.9	0.8	-85.4	0.7
spot 3	-36.7	2.0	-41.6	5.0	(VIS) 2			-81.5	0.8
spot 4	-23.2	2.5	-26.7	2.3	(UV) 2			-84.9	0.8
spot 5 (VIS)	-15.0	1.8	-16.8	1.4	(VIS) 3			-83.6	0.6
(UV)	-16.0	1.8	-18.0	2.3	(UV) 3			-84.8	0.6
spot 6 (VIS)	-23.3	1.4			spot 2 (VIS)			-70.6	1.1
(UV)	-18.4	1.3			(UV)			-75.4	1.2
(VIS) 2	-18.2	2.8			(VIS) 2			-69.1	1.2
(UV) 2	-18.9	2.8			(UV) 2			-71.4	1.1
(VIS) 3	-19.5	1.7			(VIS) 3			-67.7	1.4
(UV) 3	-18.5	2.8			(UV) 3			-70.7	0.8
					spot 3 (VIS)			-96.9	1.3
					(UV)			-100.6	4.3
					(VIS) 2			-96.9	1.3
					(UV) 2			-98.4	3.0
					(VIS) 3			-94.0	1.1
					(UV) 3			-96.6	0.9
range (VIS)	15–37		17–42					68–97	
range (UV)	16–19							71–101	
difference	1–5		1			4.5		1–5	

Table 4.3. **Summary of the average adhesion strengths of micro-structured PDMS films with preload forces of 100 mN and 200 mN with and without 0.25 wt-% spiropyran 1. Average values and standard deviations (SD) are reported for various spots on the sample as well as alternating visible light (>530 nm) and UV light (365 nm) cycles. [83]**

micro-structured									
	non-doped					0.25 wt-% spiropyran			
	100 mN preload		200 mN preload			100 mN preload		200 mN preload	
	average (mN)	SD	average (mN)	SD		average (mN)	SD	average (mN)	SD
spot 1	-94.7	1.6	-73.0	2.6	spot 1 (VIS)	-124.1	1.2	-142.7	1.5
spot 2	-98.7	1.0	-97.0	7.2	(UV)	-128.2	0.8	-144.2	4.2
spot 3	-75.9	1.9	-93.1	2.2	(VIS) 2	-122.3	0.7	-140.1	1.1
spot 4 (VIS)	-79.0	4.5	-68.9	1.7	(UV) 2	-126.0	0.6	-145.6	1.2
(UV)	-80.4	2.2	-66.1	2.3					
spot 5 (VIS)	-52.7	2.5	-78.6	2.4	spot 1 (VIS)	-87.4	1.8		
(UV)	-55.1	1.4	-76.7	2.4	(UV)	-96.1	2.0		
(VIS) 2	-51.2	1.4			spot 2 (VIS)	-89.1	1.3		
(UV) 2	-43.7	0.5			(UV)	-91.5	1.4		
spot 6 (VIS)	-71.3	3.2	-78.2	3.6	spot 3 (VIS)	-75.4	1.2		
(UV)	-73.3	2.9	-79.6	1.5	(UV)	-80.0	2.6		
(VIS) 2	-107.6	9.1	-78.0	2.4	spot 4 (VIS)	-84.2	1.4		
(UV) 2	-77.7	3.4	-79.3	1.9	(UV)	-92.1	1.1		
spot 7 (VIS)	-62.3	3.4	-107.2	6.1	spot 5 (VIS)	-63.5	1.5		
(UV)	-58.6	2.4	-99.7	5.9	(UV)	-67.2	1.9		
(VIS) 2	-60.4	2.6	-81.2	3.0					
(UV) 2	-63.0	3.0	-78.9	3.9	spot 1 (VIS)	-102.0	1.4		
(VIS) 3	-95.2	2.8	-57.9	8.7	(UV)	-106.0	1.6		
(UV) 3	-95.5	3.5	-58.6	8.3	(VIS) 2	-104.2	1.5		
					(UV) 2	-104.7	1.6		
					(VIS) 3	-102.3	2.2		
					(UV) 3	-105.8	1.2		
					(VIS) 4	-101.2	1.6		
					(UV) 4	-104.2	1.4		
					(VIS) 5	-102.5	1.5		
					(UV) 5	-103.7	1.2		
range (VIS)	51–108		58–107			64–124		140–143	
range (UV)	44–96		59–100			67–128		144–146	
difference	1–35		1–50			2–33		1–5	

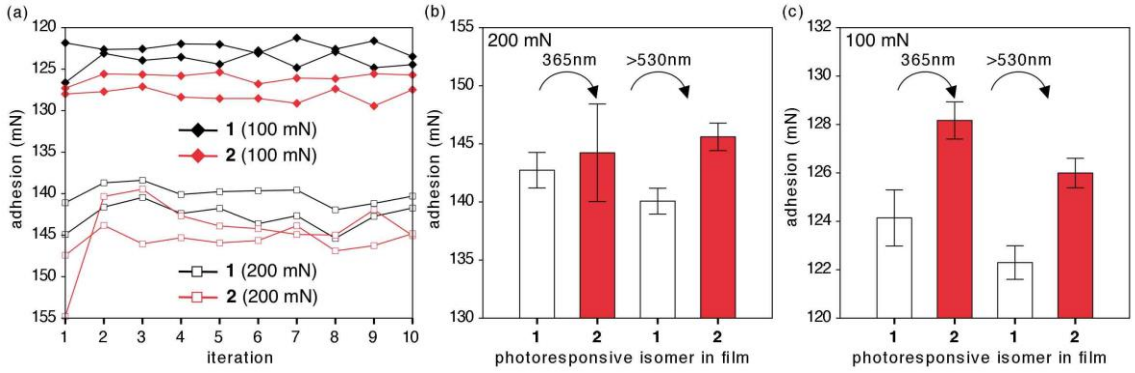

Figure 4.6. **(a) The adhesion strengths for a micro-structured PDMS film doped with spiropyran 1 (0.25 wt-%) as it is exposed to visible light (>530 nm) (black) and UV light (365 nm) (red) using preload forces of 100 mN and 200 mN. Each data point (iteration) corresponds to a single measurement on the same spot. (b,c) Average adhesion strengths for the same film before (white) and after (red) irradiation with UV (365 nm) light at the two different preload values. Note that the scale of figure (b) ranges from 130mN-155mN and (c) ranges from 120mN-132mN. [83]**

The range of adhesion strengths is highly dependent on where the measurements are made on the film. Every new spot on the same film sampled has a different adhesion (values of F_a range from 50 to 130 mN for these films), which is likely due to defects in the microstructures such as missing or folded 'mushroom caps'. The reason for the large range of adhesion strengths for non-structured films is less clear (values of F_a range from 15 to 40 mN for these films) and may be due to variations in the thickness of the film and a higher sensitivity to the preload force [42, 82].

The effect of light on the un-doped PDMS (either non-structured or micro-structured) was insignificant and the changes were not systematic when exposed to UV or visible light (Figures 4.7 and 4.8). Note that the changes were smaller than the error in the measurements. As expected, the micro-structured films had on average higher adhesive strengths than the non-structured films (almost double on average for un-doped films). Light had a significant effect on both non-structured and micro-structured films containing 0.25 wt-% spiropyran **1** (Figures 4.5 (c–e), Figure 4.9 and 4.10) using a 100 mN preload force. Figure 4.11 graphs the adhesion strengths throughout various light cycles at a single spot for a micro-structured PDMS film doped with spiropyran **1** (0.25 wt-%) as it is exposed to visible light (>530 nm) (black) and UV light (365 nm) (red) using a

preload force of 100 mN. This highlights that there is no significant fatigue occurring throughout the cycles at this spot.

For the non-structured films, the adhesion strengths increased 22% when the colorless films were exposed to UV light (365 nm) for 60 seconds. As was observed for the un-doped PDMS films, the adhesive strengths of the micro-structured films containing spiropyran **1** (0.25 wt-%) was significantly larger on average than the non-structured doped films (Tables 4.2 and 4.3). It is important to note that Increasing the doping levels of the photo-responsive compound to 0.5 wt-% had little effect on the changed in adhesive strengths (Figure 4.12).

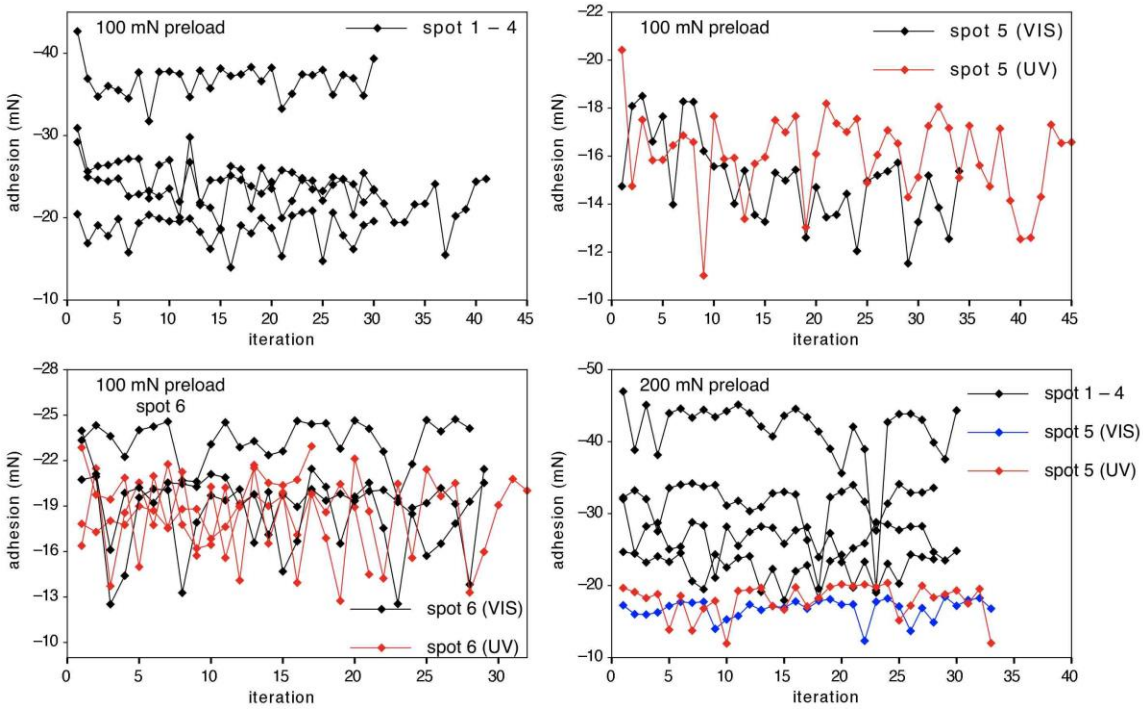

Figure 4.7. Comparison of the adhesion strengths for an un-doped, pure, non-structured PDMS film exposed to UV light (365 nm) or yellow light (>530 nm) with preload forces of 100 mN and 200 mN. Only spots 5 and 6 were exposed to the different wavelengths of light. Spots 1, 2, 3 and 4 were only measured under visible light exposure. Each 'iteration' represents a single measurement of the force required to detach the probe tip from the film at the same spot as shown in Figure 4-5 (b). [83]

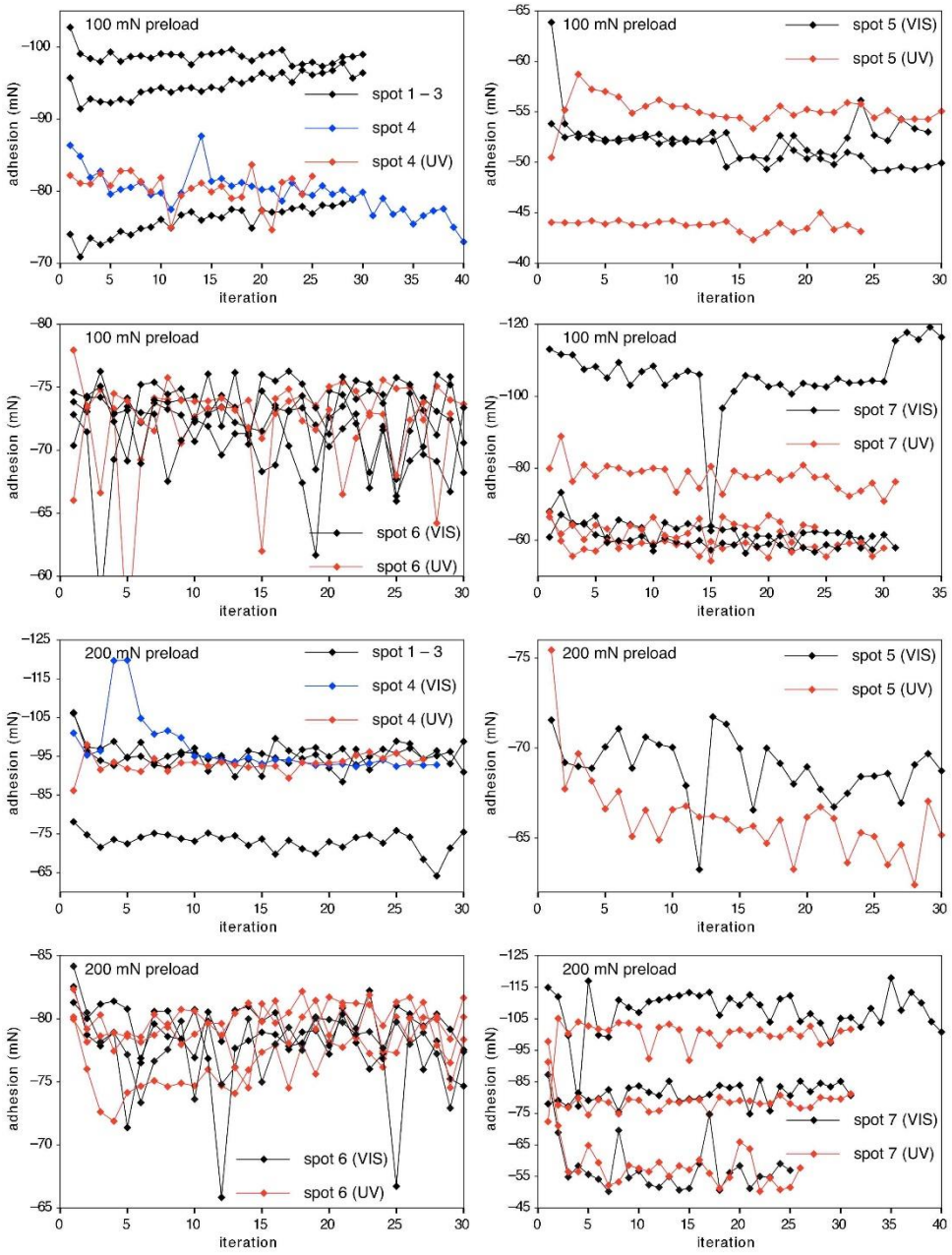

Figure 4.8. **The adhesion strengths for an un-doped (pure) micro-structured PDMS film exposed to UV light (365 nm) or yellow light (>530 nm) with preload forces of 100 mN and 200 mN. Only spots 4, 5, 6 and 7 were exposed to the different wavelengths of light. Spots 1, 2 and 3 were only measured under visible light exposure. Each 'iteration' represents a single measurement of the force required to detach the probe tip from the film at the same spot as shown in Figure 4-5 (b). [83]**

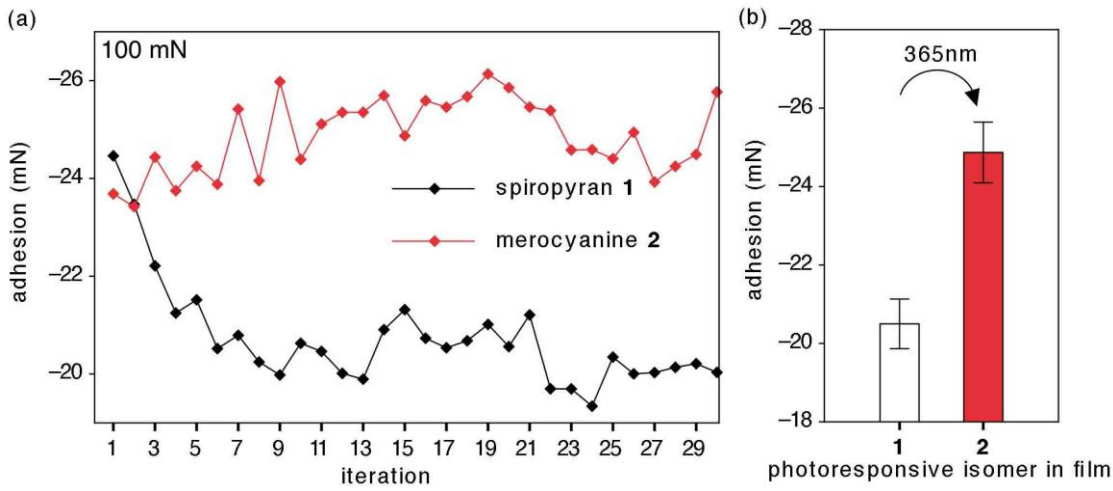

Figure 4.9. **(a) Adhesion strengths for a non-structured PDMS film doped with spiropyran 1 (0.25 wt-%) as it is exposed to visible light (>530 nm) (black) and UV light (365 nm) (red) using a preload force of 100 mN. Each data point (iteration) corresponds to a single measurement on the same spot as shown in Figure 4-5 (b). (b) Average adhesion strengths for the same film before (white) and after (red) irradiation with UV (365 nm) light for 60 seconds. [83]**

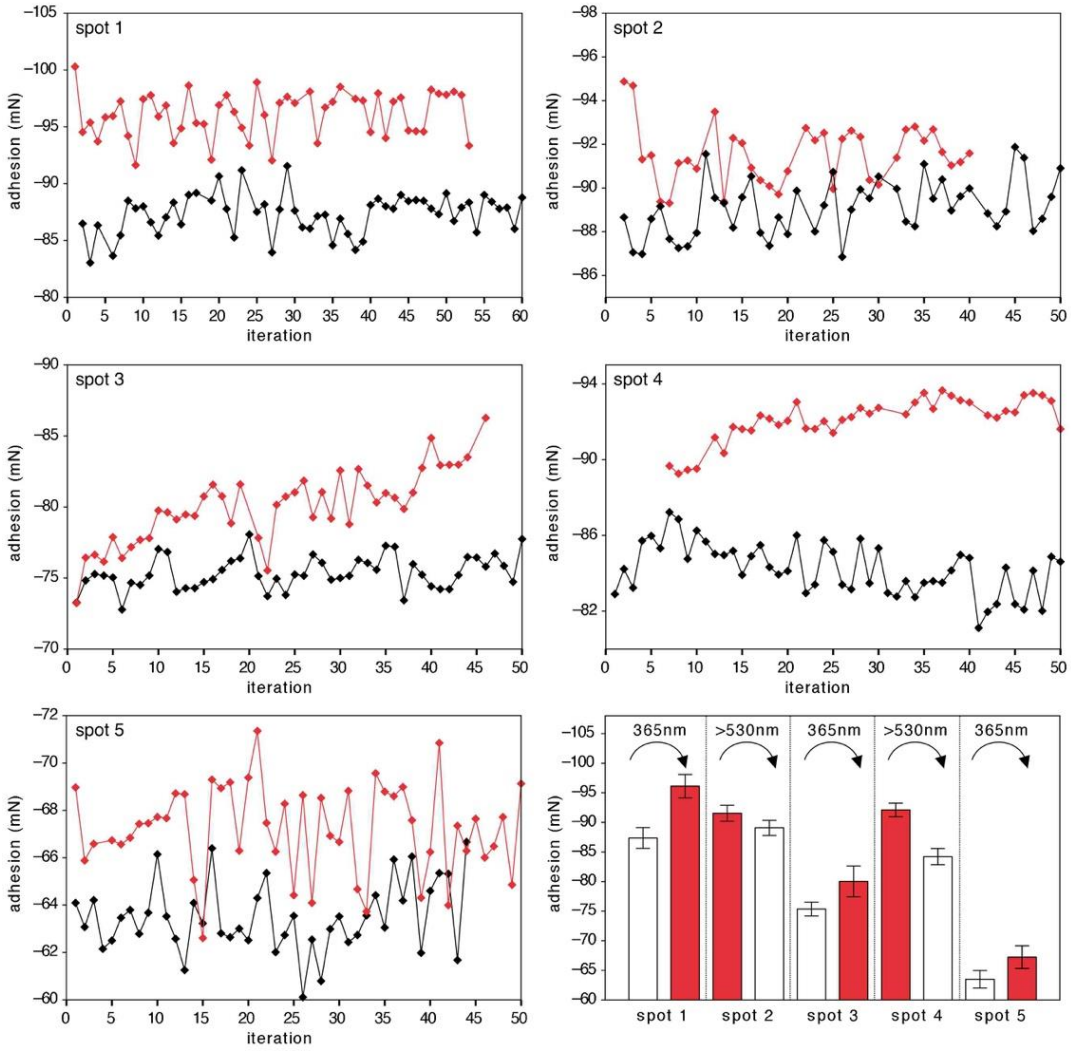

Figure 4.10. The adhesion strengths for a micro-structured PDMS film doped with spiropyran 1 (0.25 wt-%) as it is exposed to visible light (>530 nm) (black) and UV light (365 nm) (red) using a preload force of 100 mN. Each data point (iteration) corresponds to a single measurement on the same spot as shown in Figure 4-5 (b). The average values are shown in the bottom, right panel. [83]

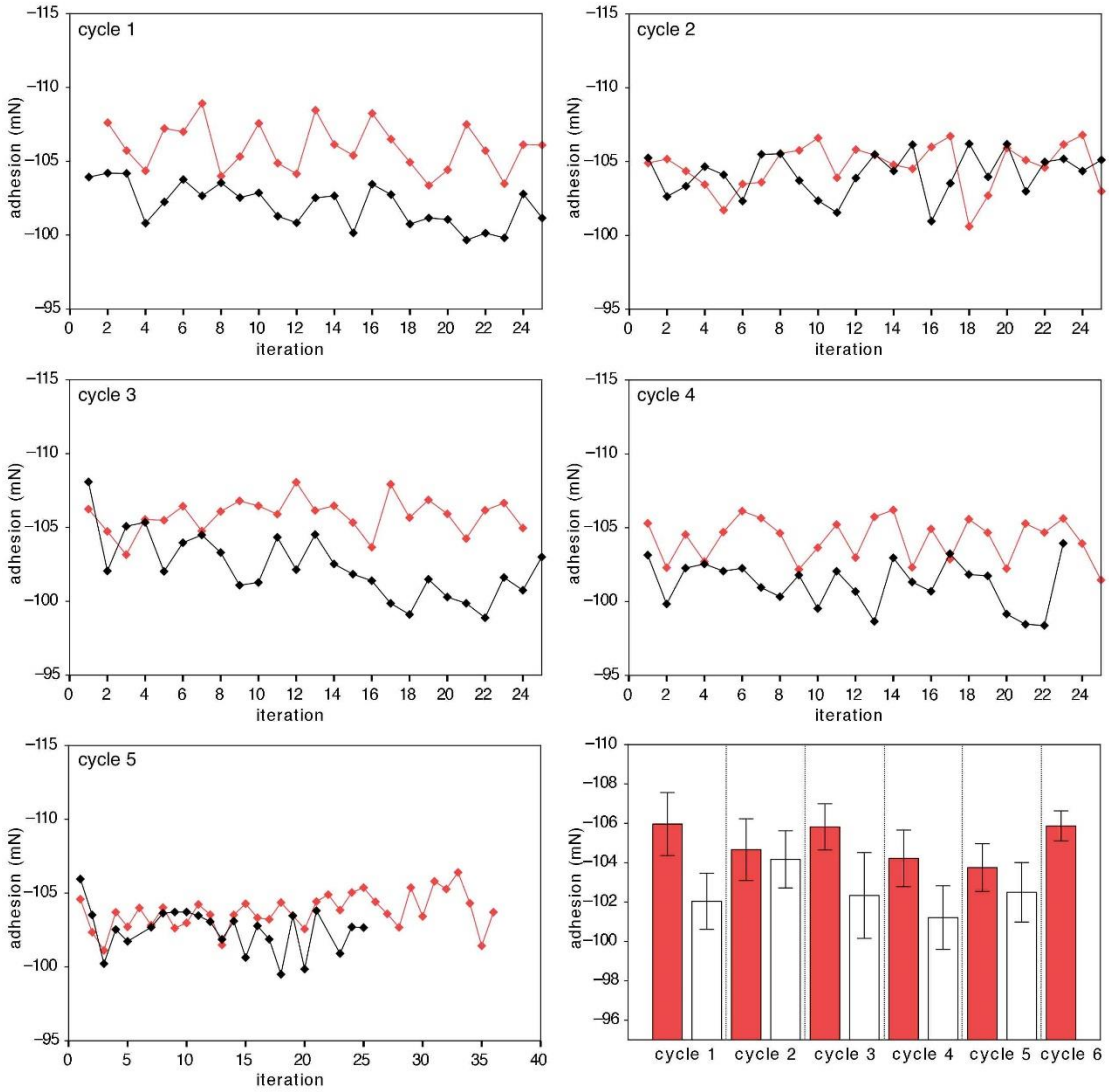

Figure 4.11. **The adhesion strengths at one single spot for a micro-structured PDMS film doped with spiropyran 1 (0.25 wt-%) as it is exposed to visible light (>530 nm) (black) and UV light (365 nm) (red) using a preload force of 100 mN. Each data point (iteration) corresponds to a single measurement on the same spot as shown in Figure 4-5 (b). The average values are shown in the bottom, right panel.**

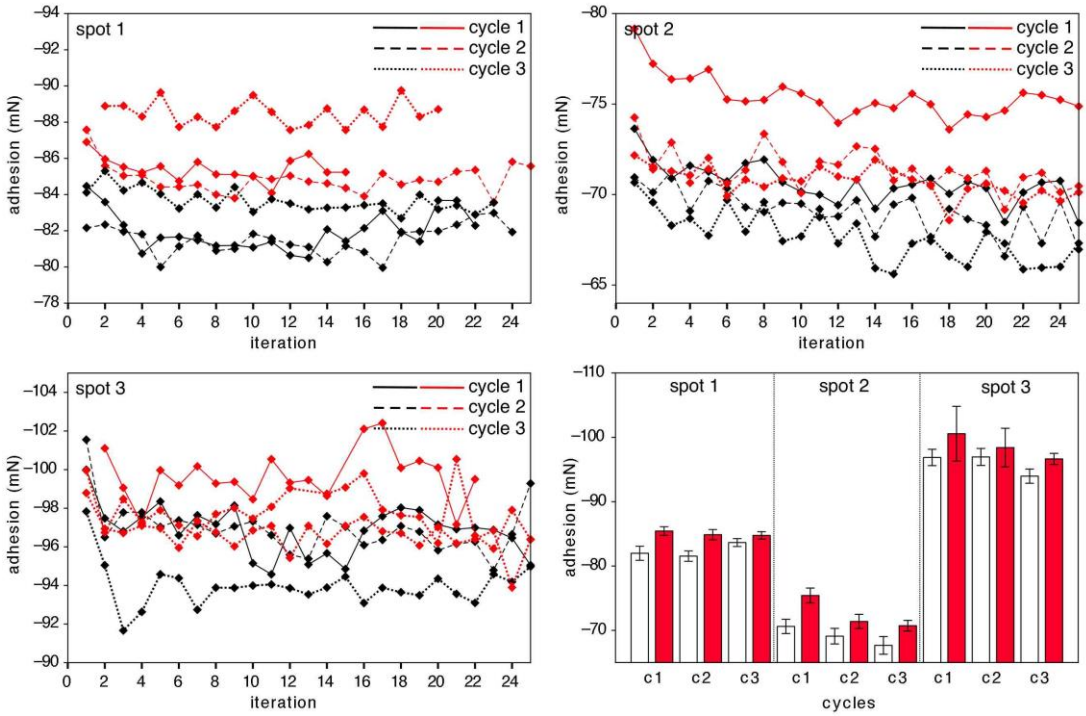

Figure 4.12. The adhesion strengths for a micro-structured PDMS film doped with spiropyran 1 (0.5 wt-%) as it is exposed to visible light (>530 nm) (black) and UV light (365 nm) (red) using a preload of 100 mN. Each data point (iteration) corresponds to a single measurement on the same spot as shown in Figure 4-5 (b). The average values are shown in the bottom, right panel.

As illustrated in Figure 4.5 (d), exposing the micro-structured films to UV light (365 nm) had a significant effect on the average values of F_a for several spots sampled throughout the film. In this experiment, the film was originally exposed to visible light (>530 nm) to ensure the photo-responsive chromophores were in their neutral spiropyran states (**1**). After the adhesion force was measured, the entire film was irradiated for 60 s with UV light (365 nm) turning it magenta as the spiropyran ring-opens to its charged merocyanine isomer (**2**). The average value of F_a was measured to be 10% larger than the original value. Moving to a new spot resulted in a different value of F_a as expected. Exposing the film to visible light (>530 nm) returned the film to its colorless state and lowered the value of F_a. This cycling between light sources was continued for a total of 5 spots on the same micro-structured film. In all cases, the magenta, merocyanine-containing film showed significant increases in the adhesion strengths.

A similar trend was observed when a single spot was cycled between its colorless neutral (**1**) state and its magenta charged (**2**) state as shown in Figure 4.5 (e). Although there are some examples that lie outside the averages, the trend is clear – the film containing the zwitterionic merocyanine isomer has an increased adhesion compared to those containing the neutral spiropyran isomer. The inconsistencies between cycles may be due to mechanical issues such as 'mushroom caps' that have not retained their shape, inconsistent photo-stationary states of the photochromic compounds within the polymer film or irregularities in the instrument's load cell. The inconsistencies are unlikely due to the spontaneous ring-closing of the merocyanine back to the spiropyran as this reaction is slow in both non-structured and micro-structured PDMS films. In the dark, the half-life for the decay of the absorption at 550 nm corresponding to compound **2** is 45–55 min for either film (Figure 4.2).

Chapter 5. Conclusion

In this report, we demonstrate how photo-responsive compounds doped into PDMS microstructures can reversibly regulate the adhesive properties of polymer films using two colors of light. As little as 0.25 wt-% of the photochromic compound had significant effects.

Despite the progress in this field, there is still much difficulty in producing fully controllable switchable materials. More specifically, the term “switchable” is here used to describe an adhesive that goes from a sticky state to a non-sticky or lower-sticky state in which the adhesion has a reduced strength compared to its original condition. This work is the initial investigation of a series of extensive experiments to fully characterize and acquire in depth knowledge on dry switchable adhesive polymers. To establish a proof of concept and ultimately advance dry adhesion technology, we have simply mixed spiropyran switch molecules in a 10:1 PDMS at a concentration of 0.25%. Samples with mushroom-cap microstructures have been fabricated as well as unstructured flat ones. The effects on the surface properties of the adhesive polymer have been reported.

Quick and efficient switching, confirmed by the optical absorption spectrum, enables control over the sample’s material properties. When the molecule is switched to the MC charged form, stronger adhesion (of about 4mN) is observed over the SP neutral form. In general, integrating this molecule increases the normal adhesion of the material of unstructured samples by a factor of ~4 for the SP state and ~5 for the MC one. Surface charge and contact angle measurements further confirm the proper functionality of the switch inside the PDMS polymer. The MC form has approximately 1.15 times more surface charges than the neutral SP one and accordingly has a lower contact angle indicating that it is more hydrophilic.

All these results give promising evidence of the control one can have over PDMS polymer by simply doping it. Following this project, the results have been published in [83]. Future generations of these ‘smart’ materials will include photochromic compounds tethered to the polymer backbone to increase loading and subsequent light-induced charge generation. In order to get the most effective switching behaviour from our polymer,

it is necessary for the SP switch to be covalently attached to the main chain of its host. This will be the next step of this work and similar studies will be performed to fully understand the fundamental interaction dynamics of this switchable material.

References

[1] J. Kinloch (1987), *Adhesion and Adhesives*: Science and Technology. Chapman and Hall, London.

[2] D. E. Packham (2005), *Handbook of Adhesion*, John Wiley & Sons Ltd, Hoboken.

[3] H. Lee, B. P. Lee, P. B. Messersmith, *Nature* **2007**, *448*, 338.

[4] M. Henrey, J. P. Diaz Tellez, K. Wormnes, L. Pambaguian, C. Menon, *Aerosp. Sci. Technol.* **2013**, *29*, 185.

[5] K. Autumn, M. Sitti, Y. A. Liang, A. M. Peattie, W. R. Hansen, S. Sponberg, T. W. Kenny, R. Fearing, J. N. Israelachvili, R. J. Full, *Proc. Natl. Acad. Sci. U.S.A.* **2002**, *99*, 12252.

[6] P. Prokopovich, V. Starov, *Adv. Colloid Interface Sci.* **2011**, *168*, 210.

[7] W. L. Noderer, L. Shen, S. Vajpayee, N. J. Glassmaker, A. Jagota, C. Y. P. Hui, *Proc. R. Soc. A* **2007**, *463*, 2631.

[8] K. Autumn, Y. A. Liang, S. T. Hsieh, W. Zesch, W. P. Chan, T. W. Kenny, R. Fearing R. J. Full, *Nature* **2000**, *405*, 681.

[9] A. Pattantyus-Abraham, J. Krahn, C. Menon, *Front. Bioeng. Biotech.* **2013**, 1, 1.

[10] E. Arzt, S. Gorb, R. Spolenak, *PNAS* **2002**, 100, 19, 10603–10606.

[11] Y. Yu, M. Nakano and T. Ikeda, *Nature* **2003**, 425, 6954, 145.

[12] R. Wang, K. Hashimoto, A. Fujishima, M. Chikuni, E. Kojima, A. Kitamura, M. Shimohigoshi, and T. Watanabe, *Nature* **1997**, 388, 431-432.

[13] A. Koçer, M. Walko, W. Meijberg and B. L. Feringa, *Science* **2005**, 309, 5735, 755-758.

[14] X. Feng, L. Feng, M. Jin, J. Zhai, L. Jiang and D. B. Zhu, *J. Am. Chem. Soc.* **2004**, 126, 62-63.

[15] J. Lahann, S. Mitragotri, T. Tran, H. Kaido, J. Sundaram, I. S. Choi, S. Hoffer, G. A. Somorjai, and R. Langer, *Science* **2003**, 299, 5605, 371-374.

[16] B. S. Gallardo, V. K. Gupta, F. D. Eagerton, L. I. Jong, V. S. Craig, R. R. Shah and N. L. Abbott, *Science* **1999**, 283, 5398, 57-60.

[17] G. B. Crevoisier, P. Fabre, J. M. Corpart and L. Leibler, *Science* **1999**, 285, 1246-1249.

[18] T. Sun, G. Wang, L. Feng, B. Liu, Y. Ma, L. Jiang and D. Zhu, *Angew. Chem., Int. Ed.* **2004**, 43, 357-360.

[19] Q. Fu, G. V. R. Rao, S. B. Basame, D. J. Keller, K. Artyushkova, J. E. Fulghum and G. P. Lopez, J*. Am. Chem. Soc*. **2004**, 126, 8904-8905.

[20] S. Minko, M. Muller, M. Motornov, M. Nitschke, K. Grundke and M. Stamm, *J. Am. Chem. Soc*. **2003**, 125, 13, 3896-3900.

[21] J. R. Matthews, D. Tuncel, R. M. J. Jacobs, C. D. Bain and H. L. Anderson, *J. Am. Chem. Soc*. **2003**, 125, 21, 6428-6433. .

[22] M. Yamada, M. Kondo, J.-I. Mamiya, Y. Yu, M. Kinoshita, J. C. Barrett, T. Ikeda, *Angew. Chem. Int. Ed.* **2008**, *47*, 4986.

[23] S. Das, P. Ranjan, P. S. Maiti, G. Singh, G. Leitus, R. Klajn, *Adv. Mater.* **2013**, *25*, 422.

[24] O. Breidbach, *Mikrokosmos* **1980**, 69, 200–201.

[25] H. Schliemann, *Funkt*. *Biol. Med*. **1983**, 2, 169–177.

[26] K. L. Johnson, K. Kendall and A. D. Roberts, *Proc. R. Soc. Lond. A* **1971**, 324, 1558, 301-313.

[27] N. J. Glassmaker, A. Jagota, C. Hui, W. L. Noderer and M. K. P. Chaudhury,, *Natl. Acad. Sci. USA* **2007**, 104, 26, 10786-10791.

[28] M. T. Northern and K. L. Turner, *Nanotechnology* **2005**, 16, 1159-1166.

[29] K. Geim, S. V. Dubonos, I. V. Grigorieva, K. S. Novoselov, A. A. Zhukov and S. Y. Shapoval (**2003**), *Nature Materials*, 2, 7, 461–463.

[30] N. J. Glassmaker, A. Jagota, C. –Y. Hui and J. Kim, *J. Royal Soc. Interface* **2004**, 1, 23–33.

[31] Y. Zhao, T. Tong, L. Delzeit, A. Kashani, M. Meyyappan and A. Majumdar,, *Journ. Vacuum Sci. Technol. B* **2006**, 24, 1, 331–335.

[32] P. Dickrell, S. Sinnott, D. Hahn, N. Raravikar, L. Schadler, P. Ajayan and W. Sawyer, *Tribology Lett.* **2005***,* 18, 1, 59–62.

[33] C. Majidi, R. E. Groff, Y. Maeno, B. Schubert, S. Baek, B. Bush, R. Maboudian, N. Gravish, M. Wilkinson, K. Autumn and R. S. Fearing, *Phys. Rev. Lett*. **2006**, 97, 7, 076103.

[34] M. Sitti and R. S. Fearing, *J. Adhesion Sci. Technol*. **2003**, 17, 8, 1055–1074.

[35] C. Menon, M. Murphy and M. Sitti, *Proc. Of the IEEE Int. Conf. on Robotics and Biomimetics* **2004**, pp. 431–436, Shenyang, China.

[36] S. Gorb, M. Varenberg, A. Peressadko and J. Tuma, *J. Royal Soc. Interface* **2007**, 4, 13, 271–275.

[37] D. S. Kim, H. S. Lee, J. Lee, S. Kim, K. –H. Lee, W. Moon and T. H. Kwon, *Microsystem Technologies* **2007**, 13, 5, 601–606.

[38] G. L. Spina, C. Stefanini, A. Menciassi and P. Dario, J. *Micromech. Microeng*. **2005**, 15, 1576–1587.

[39] A. Del Campo, C. Greiner and E. Arzt, *Langmuir* **2007**, 23, 20, 10235-10243.

[40] C. Greiner, A. Del Campo and E. Arzt, *Langmuir* **2007**, 23, 7, 3495-3502.

[41] S. Kim and M. Sitti, *Appl. Phys. Lett*. **2006**, 89, 261911.

[42] S. Kim, M. Sitti, C. Y. Hui, R. Long and A. Jagota, *Appl. Phys. Lett*. **2007**, 91, 161905.

[43] E. P. Chan, C. Greiner, E. Arzt and A. J. Crosby, *MRS Bull*. **2007**, 32, 496-503.

[44] B. Aksak, M. P. Murphy and M. Sitti, *Langmuir* **2007**, 23, 6, 3322–3332.

[45] S. N. Gorb, M. Sinha, A. Peressadko, K. A. Daltorio and R. D. Quinn, *Bioinspir. Biomimetic*. **2007**, 2, 4, S117–25.

[46] V. Spuskanyuk, R. M. McMeeking, V. S. Deshpande and E. Arzt, *Acta Biomater*. **2008**, 4, 1669–76.

[47] M. Irie, *Chem. Rev*. **2000**, 100, 1685–1716.

[48] O. Chovnik, R. Balgley, J. R. Goldman and R. Klajn, *J. Am. Chem. Soc*. **2012**, 134, 19564–19567.

[49] R. Klajn, K. J. M. Bishop, M. Fialkowski, M. Paszewski, C. J. Campbell, T. P. Gray and B. A. Grzybowski, *Science* **2007**, 316, 5822, 261–264.

[50] R. Klajn, K. P. Browne, S. Soh and B. A. Grzybowski, *Small* **2010**, 6, 13, 1385–1387.

[51] H. M. D. Bandara and S. C. Burdette, *Chem. Soc. Rev*. **2012**, 41, 1809–1825.

[52] J. Henzl, M. Mehlhorn, H. Gawronski, K. H. Rieder and K. Morgenstern, *Angew. Chem., Int. Ed.* **2006**, 45, 603–606.

[53] W. Fuss, C. Kosmidis, W. E. Schmid and S. A. Trushin, Angew. Chem. **2004**, Int. Ed., 43, 4178–4182.

[54] J. Zhang, J. K. Whitesell and M. A. Fox, Chem. Mater. **2001**, 13, 7, 2323–2331.

[55] V. I. Minkin, *Chem. Rev.* **2004**, 104, 2751–2776

[56] R. Guglielmetti. *Photochromism: Molecules and Systems* **2003**, ed. H. Durr and H. Bouas-Laurent, Elsevier, Amsterdam.

[57] R. C. Bertelson, *In Organic Photochromic and Thermochromic. Compounds, ed. J. C. Crano and R. J. Guglielmetti* **2002**, Kluwer Academic Publishers, New-York.

[58] K. Matsuda and M. Irie, *J. Photochem. Photobiol*. **2004**, C, 5, 2, 169–182.

[59] T. Kudernac, S. J. van der Molen, B. J. van Wees and B. L. Feringa, *Chem. Commun.* **2006**, 34, 3597–3599.

[60] Y. Chen, C. M. Wang, M. G. Fan, B. L. Yao and N. Menke, *Opt. Mater*. **2004**, 26, 1, 75–77.

[61] B. Heinz, S. Malkmus, S. Laimgruber, S. Dietrich, C. Schulz, K. Rueck-Braun, M. Braun, W. Zinth and P. Gilch, J*. Am. Chem. Soc*. **2007**, 129, 8577–8584.

[62] N. Koumura, R. W. J. Zijlstra, R. A. van Delden, N. Harada and B. L. Feringa, *Nature* **1999**, 401, 152–155.

[63] M. R. di Nunzio, P. L. Gentili, A. Romani and G. Favaro, *Chem. Phys. Chem* **2008**, 9, 5, 768–775

[64] R. Klajn, *Chem. Soc. Rev.* **2014**, *43*, 148.

[65] L. Florea, D. Diamond, F. Benito-Lopez, *Macromol. Mater. Eng.* **2012**, 297, 1148.

[66] M. J. Lee, B. W. Yoo, S.T. Shin, S. R. Keum, *Dyes Pigm.* **2001**, 51, 15.

[67] F. Ercole, T. P. Davis, R. A. Evans, *Polym. Chem.* **2010**, 1, 37.

[68] H. Tachibana, Y. Yamanaka, M. Matsumoto, *J. Mater. Chem.* **2002**, 12, 938.

[69] L. Potisek, A. Davis, R. Sottos, R. White, S. Moore, *J. Am. Chem. Soc.*, **2007**, 129, 13808–13809.

[70] M. Tomasulo, S. L. Kaanumal, S. Sortino, F. M. Raymo, *J. Org. Chem.* **2007**, 72, 595–605.

[71] D. Sameoto, C. Menon, *J. Micromech. Microeng.* **2009**, 19, 115002-115002.

[72] J. Krahn, D. Sameoto, C Menon, *Smart Mater. Struct.* **2011**, 20, 015014-015014.

[73] J. Krahn, C. Menon, *Langmuir*, **2012**, *28*, 5438-5443.

[74] J. P. Diaz Tellez, *ci. China. Ser. E*, **2010**, *53*, 2942-2946.

[75] D. Sameoto, H. Sharif, C. Menon, *J. Adhes. Sci. Technol.* **2012**, *33*, 2641-2946.

[76] J. Lin, S. Qiu, K. Lewis, and A. M. Klibanov, *Biotechnol. Prog*. **2002**, 18, 5, 1082-1086.

[77] K. L. Mittal, *Contact Angle, Wettability and Adhesion* **1993**. VSP Ed., Utrecht.

[78] H. Cui, G. Z. Yang, Y. Sun, and C. X. Wang *Appl. Phys. Lett*. **2010**, 97, 183112.

[79] A. Athanassiou, M. I. Lygeraki, D. Pisignano, K. Lakiotaki, M. Varda, E. Mele, C. Fotakis, R. Cingolani, S. H. Anastasiadis, *Langmuir* **2006**, *22*, 2329

[80] S. Wang, Y. Song, L. Jiang, *J. Photochem. Photobio. C* **2007**, 8, 18-29.

[81] V. A. Parsegian, *Van der Waals Forces*, *First edition* **2006**, Cambridge University Press, Cambridge.

[82] R. Long, C.-Y. Hui, *Proc. R. Soc. A* **2009**, *465*, 961.

[83] P. Tannouri, K. M. Arafeh, J. M. Krahn, S. L. Beaupré, C. Menon, and N. R. Branda, *ACS Chem.of Mat.* **2014**, 26, 15, 4330-4333.